Study of Various TDMA Schemes for Wireless Networks in the Presence of Deadlines and Overhead

César Santiváñez, *Student Member, IEEE*, and Ioannis Stavrakakis, *Senior Member, IEEE*

***Abstract*— The objective of this paper is to determine the minimum system dropping rate (or, equivalently, dropping probability) induced by time division multiple access (TDMA) schemes supporting time-constrained applications with common maximum cell delay tolerance. Expressions are derived for the induced system dropping rate for various TDMA schemes with different overhead and the maximum number of users than can be admitted in the network without violating the maximum dropping rate constraint is determined. The system dropping rate achieved by suboptimal TDMA schemes is compared against the optimal (although ideal) TDMA scheme performance. The performance limiting factors associated with the suboptimal schemes are identified, and the magnitude of their (negative) impact is evaluated. Based on this information it is possible to point to performance improving modifications which should be pursued to the extent permitted by technological constraints. Finally, based on this derivations a network designer may choose the best TDMA scheme—among realizable variations of those considered here—to use in a particular situation.**

***Index Terms*—Adaptive time division multiple access (TDMA), deadline, dropping rate, multiaccess, overhead, quality of service, variable frame.**

I. Introduction

WIRELESS communications networks, e.g., cellular telephony, have grown in the past two decades to become a sizeable part of the telecommunications market [1]. This rapid growth is due to some highly desirable properties of a tetherless terminal, such as mobility, and has been enabled by advances in digital signal processing technology—which have lead to the reduction in size, power consumption and cost of the mobile units—and the assignment of radio spectrum for public (e.g., personal communications systems) and private (e.g., wireless LAN) wireless networks.

Two major wireless networking technologies have emerged: cellular systems (originally designed to support voice applications in a wide area network) and wireless LAN's (developed to support computer data applications in a local area network). Currently, these two technologies are converging. Cellular systems have evolved from an analog network (AMPS) to a circuit-switched based digital network (e.g., GSM) and the next generation wireless systems are expected to be multiservice cell-switched based networks. On the other hand, wireless LAN's are now expected to provide real-time services such as image, video, and possibly voice support. This convergence drives a demand for a single network architecture capable of supporting all aforementioned services in an integrated fashion, which should also be compatible with the fixed ATM-based integrated services network. For this reason, it will be natural to consider an ATM-based protocol for the local and broadband wireless network [2], [3] namely wireless ATM.

System architectures to enable "wireless ATM" (WATM) have already been developed [4]–[6]. They employ a data link control (DLC) layer to combat the unreliability of the wireless link and a medium access control (MAC) protocol to organize the sharing of the multiaccess channel. MAC's for WATM have been examined in [4] and [7]–[11]. They all employ time division multiple access (TDMA) with on-demand assignment of the transmission resources by a central agent or *scheduler*. It is believed that a TDMA-based MAC provides the best mix of cost, range, interference and performance [12].

Since the wireless channel is a medium shared by distributed users, its allocation presents some distinct problems from those associated with the allocation of outgoing link resources to arrivals to a fixed network node. In the latter case, the scheduler has complete knowledge of the demand for resources as soon as they are generated (occurrence of incoming link arrivals). In addition, scheduling decisions (resource assignments) can be implemented instantaneously, due to the collocation of the scheduler and the workload in the fixed node. In a dynamic wireless environment though, the scheduler needs to be communicated by the distributed users of their demands for resources, as well as inform the users of its decision (slot assignment). This communication takes place at discrete points in time [4], [7]–[11], and it is not continuous due to communication resource limitations. It is implemented by employing various mechanisms such as a control channel, piggy-backing on information bearing cells, and polling procedures; such mechanisms introduce some overhead in the system.

A MAC protocol should employ a scheduler to allocate resources effectively by taking into consideration the quality of service (QoS) requirements of the supported applications. A call admission control function is assumed to be employed as well, shaping the set of the supported applications (accepted sessions). In this paper, the QoS is defined in terms of a maximum tolerable cell delay and dropping probability. A cell is dropped when its maximum tolerable delay is exceeded,

Manuscript received August 31, 1998; revised March 19, 1999. This work was supported in part by a Fulbright Scholarship, the National Science Foundation under Grant NCR-9628116, and the GTE Corporation.

C. Santiváñez is with the Department of Electrical and Computer Engineering, Northeastern University, Boston, MA 02115 USA (e-mail: cesar@cdsp.neu.edu).

I. Stavrakakis was with the Department of Electrical and Computer Engineering, Northeastern University, Boston, MA 02115 USA. He is now with the Department of Informatics, University of Athens, Athens 15784 Greece.

Publisher Item Identifier S 0733-8716(99)05638-3.

0733–8716/99$10.00 © 1999 IEEE

or, equivalently, when its remaining delay tolerance reaches zero and its service is not completed; the remaining delay tolerance is equal to the maximum delay tolerance when the cell is generated and decreases by one in every subsequent slot (cell service time unit). Such QoS parameters are typically associated with real-time applications such as voice and video.

In a real wireless network, there are two other causes for cells being dropped: a higher bit error rate due to the wireless channel and handoffs due to the user's mobility. A complete analysis of QoS guarantees in wireless ATM network should necessarily include these different causes of cell being dropped. Such an analysis is complex and is out of the scope of the present paper. However, it should be noticed that the three different causes of cells being dropped obey to different mechanisms. Cells being dropped at a handoff depend on mobility pattern and number of users in the network. The probability of transmission error will depend on the noise and characteristics of the channel (i.e., memoryless, flat fading, etc.). The number of cells dropped because their delay in accessing the medium was greater than their maximum delay tolerance (deadline expiration) depends on the variability of the aggregated traffic. The present work is oriented toward understanding the mechanism involved in the dropping of cells due to deadline expiration. This understanding is fundamental to network designers, especially in wireless ATM networks.

An ATM network is expected to support different classes of traffic. The analysis of a system with sources of different classes is also complex and out of the scope of the presented paper. Constant bit rate (CBR) sources does not require overhead in coordination with the central station and available bit rate (ABR) and unspecified bit rate (UBR) sources do not have a deadline. Only variable bit rate (VBR) sources present both characteristics: variability in the traffic and having a maximum delay tolerance. Therefore, VBR sources are the best choice to study the mechanisms governing the dropping of cells due to delay expiration. After this understanding is gained, it is easier to a network designer to provide a solution that also handles CBR, ABR, and UBR sources. Therefore, in the present paper VBR-like sources were considered. The additional assumption that the sources were memoryless was made to allow a mathematically tractable solution.

The objective in this paper is to determine the minimum *system* dropping rate (or, equivalently, dropping probability) induced by various TDMA schemes supporting time-constrained applications with common maximum cell delay tolerance. Based on these derivations, the optimal (or of largest "capacity") TDMA scheme—among those considered—will be determined, which is another objective of this study. From the study of these TDMA schemes it will be possible to identify the performance limiting factors associated with the suboptimal schemes, determine the magnitude of their (negative) impact and to point to performance improving modifications which should be pursued to the extent permitted by technological constraints.

For the minimum system dropping rate to be induced in a TDMA scheme, the employed scheduler must try to minimize the number of cells dropped per unit time (slot). In the environment with time constrained applications considered here this scheduler will be the one implementing the shortest time to extinction (STE) service discipline [13], that is, serving cells in the order of increasing remaining delay tolerance and dropping expired (zero delay tolerance) cells. It is clear that the STE service discipline is similar to the earliest due date (EDD) service discipline (proposed in [15] and [16]) in that it will never schedule a cell with a later due date (expiration time) before another cell with an earlier due date (expiration time). EDD may schedule a cell, however, who's due date has already past. Scheduling such an expired cell—that is no longer useful—may result in waste of bandwidth and it is suboptimal. STE will always discard such an (expired) cell. Any attempt to deviate from the STE service discipline—to control delay jitter, establish some type of fairness, diversify the induced dropping rate, etc.—can only increase the resulting (overall) system dropping rate [13], [14]. For this reason, the STE service discipline will be assumed to be employed by the scheduler in all TDMA schemes considered here, to induce the minimum dropping rate possible. As it will be pointed out later, some deviation from the STE service discipline which does not increase the induced dropping rate is easily recognizable for certain TDMA schemes. Finally, it should be noted that all schemes considered here are work conserving except for the fixed frame length TDMA scheme.

The first TDMA scheme (Section II)—referred to as the ideal continuous entry TDMA (ICE-TDMA) scheme—is equivalent to a (centralized) dynamic TDM as it would be employed in a fixed network node. No frame structure is present and the scheduler is assumed to have knowledge of all past arrivals at the time when they occur. Thus, cells are considered by the scheduler as soon as they are generated (continuous entry) which would not be feasible in a wireless environment (ideal). The ICE-TDMA scheme (under the STE service discipline employed by the scheduler as indicated earlier) will be the optimal scheme against which all other—more realistic—schemes will be compared. The cell dropping rate induced by the ICE-TDMA scheme is calculated by deriving a closed form expression, as opposed to developing a numerical solution which is the case under the other TDMA schemes considered in this paper. This study provides insight into the more realistic TDMA schemes in addition to determining the lower bound on the system dropping rate under any TDMA scheme supporting the same set of applications.

The second TDMA scheme (Section III)—referred to as the ideal variable frame length TDMA (IVFL-TDMA) scheme—employs a frame structure of variable length, at the boundaries of which scheduling decisions are taken. A gated-STE service discipline is employed which starts servicing according to the STE service discipline the cells arrived before the beginning of the current frame only, until all such cells are either served or dropped, marking the end of the current frame. The scheduler is assumed to have knowledge of the exact time when past arrivals occurred when scheduling decisions are taken only, as opposed to when these arrivals occur; the latter is the case under the ICE-TDMA scheme. Consequently, the gated-STE service discipline could schedule cells differently than the STE and, thus, suboptimally. This

could be the case if an earlier arriving cell has a remaining delay tolerance greater than that of a later arriving cell at the time the later cell arrives. If such arrivals occur during different frames then the gated-STE service discipline would schedule for service the earlier cell first while the STE service discipline would schedule the later first. As a result, the performance of the gated-STE service discipline may be suboptimal. As long as always earlier arriving cells have a remaining delay tolerance less than or equal to that of a later arriving cell at the time the later cell arrives, then the scheduling decisions of the STE and gated-STE policies would coincide and the resulting system performance be identical. The above condition holds in the case in which all arrivals have the same maximum delay tolerance which is assumed to be the case in this paper.

In view of the above discussion it is evident that the system dropping rate induced under the ICE-TDMA and IVFL-TDMA schemes will be identical. Because of the delay associated with the arrival information availability to and scheduling decisions by the scheduler under the gated-STE service discipline, the IVFL-TDMA scheme is expected to be less flexible (and potentially less effective) in selecting cells to be discarded in order to meet a QoS specification requiring service discrimination or fairness, delay jitter control, etc.

Despite the fact that the system performance is identical under the ICE-TDMA and IVFL-TDMA schemes, there are several reasons justifying the presentation and study of the IVFL-TDMA scheme. First, the IVFL-TDMA scheme requires less communications overhead than the ICE-TDMA scheme: one exchange every frame versus every slot, respectively. If a separate communications channel is available and can be utilized for request/assignment exchanges between the users and the scheduler then both the ICE-TDMA and IVFL-TDMA schemes become feasible, more so the IVFL-TDMA though, due to the lesser (more realistic) information exchange overhead. Second, the IVFL-TDMA scheme is a limiting case of (or can be extended to) the real variable frame length TDMA (RVFL-TDMA) scheme (Section IV), which considers explicitly the request/assignment overhead as it is present in practical (deployed) systems. Thus, the insight gained as well as the analysis developed in the study of the IVFL-TDMA scheme are useful for the study of the RVFL-TDMA scheme. For the later analysis purposes, an alternate analysis of the IVFL-TDMA scheme is presented in Section III despite the fact that it leads to the same numerical results as the different approach developed for the study of the ICE-TDMA scheme in Section II.

The third TDMA scheme (Section IV)—referred to as the real variable frame length TDMA (RVFL-TDMA) scheme—is similar to the IVFL-TDMA scheme, only that a fixed amount of time during each frame is utilized for request/assignment exchange between the users and the scheduler and not for cell transmission (frame overhead). The RVFL-TDMA scheme is the most realistic of the three presented so far and has been employed in the wireless system developed in [11] (this system also considers overhead of variable length). In the present study the impact of the overhead is evaluated analytically by deriving tight bounds on the system dropping rate and a number of interesting comparative results are presented. Among the latter, there is a comparison of the performance induced under the RVFL-TDMA scheme and the optimal real fixed frame length TDMA (RFFL-TDMA) scheme discussed next.

The fourth TDMA scheme (Section V)—referred to as the real fixed frame length TDMA (RFFL-TDMA) scheme—assumes a fixed frame length, a fixed part of which is considered to be overhead. Tight bounds on the induced system dropping rate are derived. The case of zero frame overhead—leading to the ideal fixed frame length TDMA (IFFL-TDMA) scheme—is easily analyzed as a special case of the RFFL-TDMA scheme by setting the frame overhead equal to zero. It should be noted that a real fixed frame length TDMA (RFFL-TDMA) scheme can be a nonwork conserving scheme since empty slots may be left in a frame while cells are waiting for service.

In a RFFL-TDMA scheme the slots of the fixed frame can be preassigned to a specific application, rendering the exchange of requests/assignments between users and scheduler unnecessary. In this case the frame overhead can be eliminated, leading to the fixed frame TDMA (FF-TDMA) scheme, where the scheduler assignments are static (do not vary on-demand). This is basically the TDM scheme employed in the T-1 system for voice transmission. While the FF-TDMA scheme will outperform any other TDMA scheme under proper frame sizing and regular applications (constant traffic type of applications), it would be very inefficient in the presence of variable traffic applications. In the latter environment allocating the time slots dynamically upon demand would improve performance. Since the slots are not reserved, some communications resources will need to be utilized for the request/assignment information exchange between users and scheduler leading to a RFFL-TDMA scheme if some frame overhead is used for this communication. Thus in a dynamic traffic environment in which portion of the time—as opposed to other resource—is expended for the exchange of request/assignment information, the RVFL-TDMA and RFFL-TDMA schemes could be employed. As the results will demonstrate, the induced system dropping rate under the RVFL-TDMA scheme is lower than that under the best RFFL-TDMA scheme employing the optimal length for the fixed frame.

A discussion on the applicability and relative (comparative) effectiveness of the various TDMA schemes studied in Sections II–V is presented in Section VI along with a number of numerical results.

The common environment assumed in all TDMA schemes consists of N memoryless time-constrained applications with identical maximum delay tolerance equal to T time units; the time unit is referred to as the (time) slot and is assumed to be equal to the cell service time. The N users compete for the time resource which is allocated by the scheduler at the scheduling decision times, as indicated earlier.

II. The Ideal Continuous Entry TDMA (ICE-TDMA) Scheme

As indicated earlier, under the ICE-TDMA scheme the time-slots are (re)allocated every time a new cell arrival occurs

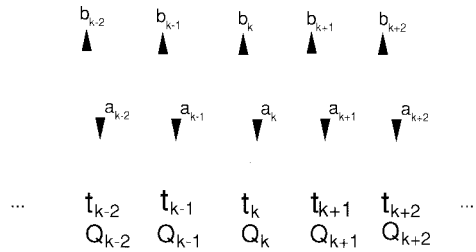

Fig. 1. Arrivals and departures at ideal continuous entry TDMA scheme.

(continuous-entry scheme). It is assumed that no time is consumed for the users to make their reservation nor for the scheduler to inform the users of its assignments (ideal scheme).

Let t_k denote the time at the beginning of the kth time slot. It is assumed that the transmission requests (namely arrivals) and the cell departures occurs at slot boundaries, that is at times $\{t_k\}$, with $k = 0, 1, \ldots, +\infty$. Without loss of generality it is also assumed that a cell transmission (if any) is completed at time t_k^- (i.e., the departure process is right-continuous) and that cell arrivals (if any) occur at t_k^+ (i.e., the arrival process is left-continuous). Fig. 1 shows a sequence of such events.

Let Q_k denote the number of cells in the system at time t_k (just after a departure but before the new arrivals); let a_k denote the number of arrivals at t_k^+; let b_k denote the number of cells departing at time t_k^- (zero or one). If a_k cells arrived at t_k^+ then the last of these cells would have to wait for $Q_k + a_k$ time slots before its transmission is completed. If this time is greater than T time slots then this cell will not meet its deadline and will be dropped. It is easy to see that the scheduler will drop $Q_k + a_k - T$ cells. Note that it is not necessary to drop the last $Q_k + a_k - T$ cells but any $Q_k + a_k - T$ cells in the buffer at time t_k^+. This is in contrast to the gated scheme (discussed later) under which only cells which have not been scheduled for transmission yet can be dropped.

The number of cells in the system at time t_{k+1} (after the last departure but before any new arrivals) is given by

$$\begin{aligned} Q_{k+1} &= \min\{T, Q_k + a_k\} - b_{k+1} \\ &= \min\{T, Q_k + a_k\} - 1_{\{\text{System_Busy}\}}. \end{aligned}$$

From the above, $0 \le Q_k \le T - 1$ for any value of k. Since $\{a_k\}$ are independent and identically distributed (i.i.d.) random variables (because the sources are memoryless), then the process $\{Q_k\}$ is a Markov process with transition matrix $\langle P_{ij} \rangle$ (i.e., $P_{ij} = P\{Q_{k+1} = i / Q_k = j\}$), derived in Appendix I-A. Then, the steady-state probability distribution of Q_k is expressed as a function of T, as shown in Appendix I-B. Using the steady-state probability distribution of Q_k and the probability distribution of the arrivals, a closed-form expression for the dropping rate is derived in Appendix I-C. It turns out that the dropping rate as a function of the maximum delay tolerance T can be described as the quotient between two IIR (infinite impulse response) filters as follows (see Appendix I-C):

$$d_r(T) = \frac{\mathcal{Z}^{-1}\{N(z)X(z)\}}{\mathcal{Z}^{-1}\{Y(z)\}}$$

where

$$\begin{aligned} N(z) &= \frac{z^{-1}[D(z) + \lambda - 1]}{1 - z^{-1}}, \\ X(z) &= \frac{l_0}{D(z)}, \qquad Y(z) = \frac{l_0 z^{-1}}{(1 - z^{-1})D(z)} \\ D(z) &= l_0 + (l_0 + l_1 - 1)z^{-1} + (l_0 + l_1 + l_2 - 1)z^{-2} \\ &\quad + \cdots + (l_0 + l_1 + l_2 + \cdots + l_{n-1} - 1)z^{-(n-1)}. \end{aligned}$$

$l_\mu = P\{a_k = \mu\}$ for $\mu = 0, \ldots, n$ is the probability of exactly μ arrivals at any point in time, and λ is the mean arrival rate, that is, $\lambda = \sum_{\mu=1}^{n} \mu l_\mu$.

This method is computationally reliable and simple, and there are available several computational tools. The previous expression is valid for different values of the mean arrival rate (λ), even greater than one. For moderate values of T such that the terms correspondent to the dominant pole r_d [largest root of $D(z)$] dominate over the other poles' terms, the dropping rates may be accurately approximated by

$$d_r(T) \approx \frac{N(r_d) r_d^{T-1}}{\dfrac{1 - r_d^{T-1}}{1 - r_d} + \dfrac{|N'(r_d)|}{N(r_d)}}. \tag{1}$$

For the case of interest, when $\lambda < 1$, for large values of the maximum delay tolerance $(T > 1/(1 - r_d))$ the dropping rate function will be dominated by an exponential function on the dominant pole r_d. Thus $d_r(T) \approx \alpha r_d^T$ where α is a constant as explained in Appendix I-C and would depend on the traffic rate, variance and "shape" [function $D(z)$]. For smaller values of T $(T < 1/(1 - r_d))$, the dropping rate will be dominated by a inversely linear function on T with constant values dependent on rate, variance and "shape" of the arrival process. When the arrival rate increases closer to one, the linear region extends for a greater set of T's and the dependence of the constants in the "shape" of $D(z)$ is decreased. In the limiting case when $\lambda = 1$, the linear region will dominate the dropping rate for all values of T and its constant values will depend only in the first three moments [and not in the "shape" of $D(z)$]. For large values of T, only the first two moments produce a significant effect in the dropping rate, which is otherwise independent of the "shape" of the arrival process.

Thus a closed-form solution for the dropping rate as a function of the maximum delay tolerance (T) is found. The same quantity will be derived again by following a different procedure in the next section where the IVFL-TDMA scheme is analyzed. Although that procedure is less insightful, it will be employed with minor modifications in the study of the RVFL-TDMA scheme (considering the frame overhead). The dropping rate computed in Section III represents the optimal (minimal) dropping rate that any TDMA scheme can achieve under the same traffic characteristics (set of supported applications).

III. The Ideal Variable Frame Length TDMA (IVFL-TDMA) Scheme

The IVFL-TDMA scheme described briefly in Section I is analyzed in this section.

Let t_k^g denote the instant of the kth scheduling decision or beginning of the kth service cycle (frame); let L_k denote the

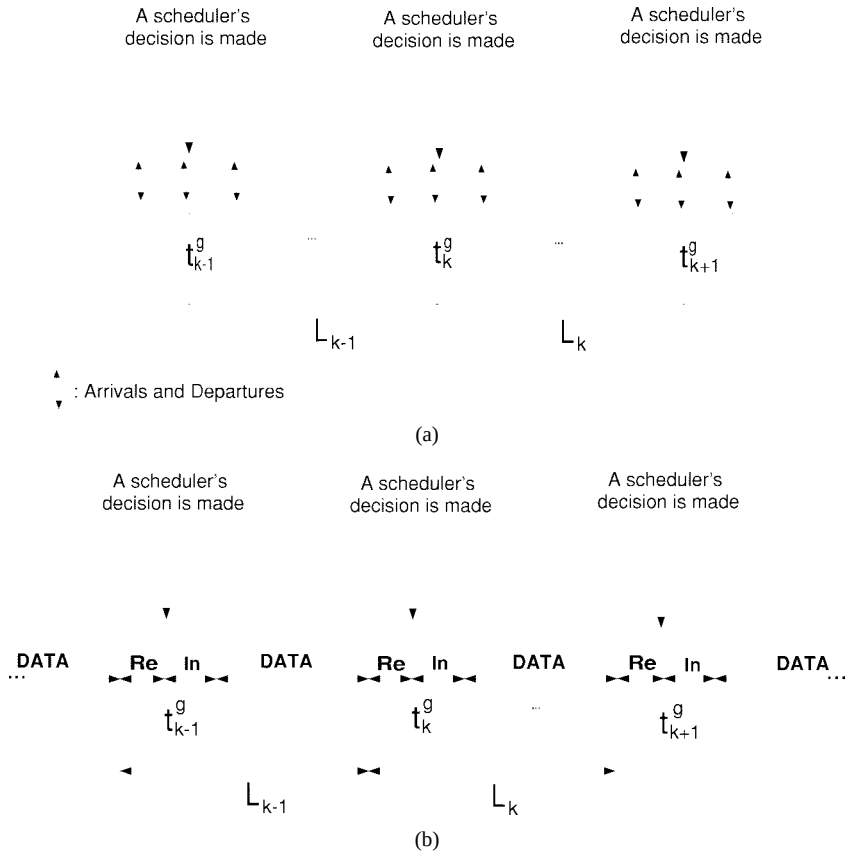

Fig. 2. Events and quantities of interest for the (a) ideal and (b) real variable frame length TDMA schemes.

length of this frame ($L_k = t^g_{k+1} - t^g_k$) as shown in Fig. 2(a). Without loss of generality, the arrival and departure processes are assumed to be right continuous. If no cell is waiting for transmission at time t^g_k, the present service cycle is empty and the next service cycle begins after one time slot. That is, an empty service cycle has a duration of one empty time slot. From the above and since any cell waiting for more than T time slots must be discarded, it follows that $1 \le L_k \le T$.

In the following sections, the dropping rate is evaluated using the following procedure: first, the conditional expected number of dropped cells in a frame given that the length of the previous frame is L, namely $\overline{d}^I_{r/L}(T)$, is computed; superscript I stands for ideal. Second, using the transition probability matrix $\langle P^I_{ij} \rangle$, describing the next frame length given the current one, the steady-state frame length probability distribution $\prod^I_i$ is calculated. Finally, the dropping rate $d^I_r(T)$ is computed from the following expression:

$$d^I_r(T) = \frac{E_L\left\{\overline{d}^I_{r/L}(T)\right\}}{E\{L\}} = \frac{\sum_{i=1}^{T} \prod^I_i \, \overline{d}^I_{r/i}(T)}{\sum_{i=1}^{T} i \prod^I_i}. \qquad (2)$$

A. Conditional Expected Number of Dropped Cells, $\overline{d}^I_{r/L}(T)$

Let $R(t)$ denote the cumulative arrivals up to (and including) time t (right continuous). Let $\hat{A}_{k-1}(\tau)$ (see Fig. 3) denote the number of arrivals between time t^g_{k-1} and $t^g_{k-1}+\tau$, that is,

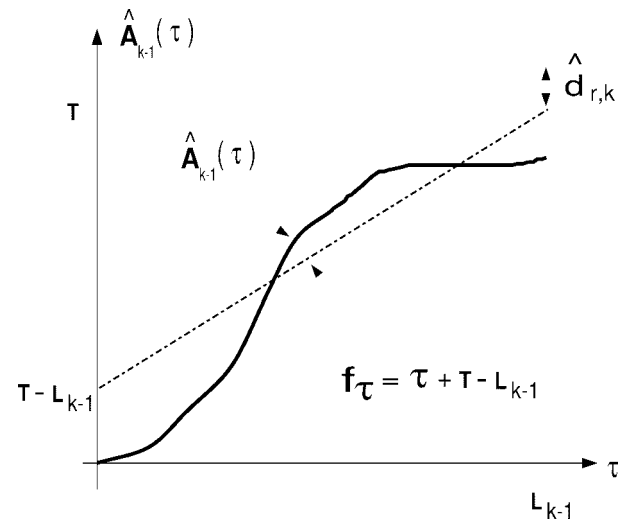

Fig. 3. Arrivals (waiting cells) during the $(k-1)$th service cycle.

τ time slots after the beginning of the previous service cycle

$$\hat{A}_{k-1}(\tau) = R(t_{k-1}+\tau) - R(t_{k-1}), \qquad 0 \le \tau \le L_{k-1}.$$

Note that since sources are assumed to be memoryless, the evolution of the process $\{\hat{A}_{k-1}(\tau)\}_{\tau=0}^{L_{k-1}}$ does not depend on time t_{k-1} but only on the length of the previous cycle, L_{k-1}; also $\hat{A}_{k-1}(0) = 0$, since the arrival process is right continuous.

At time t^g_k the scheduler considers the $\hat{A}_{k-1}(L_{k-1})$ cells waiting for transmission, schedules some of them for transmission (namely L_k) and drops the rest (namely $\hat{d}_{r,k}$).

At time $t^g_{k-1}+1$ there will have arrived $\hat{A}_{k-1}(1)$ cells, the last of which will have to wait the $L_{k-1}-1$ time slots remaining for the end of the previous service cycle, plus $\hat{A}_{k-1}(1)$ time slots to complete its transmission. If this time $(\hat{A}_{k-1}(1)-1+L_{k-1})$ is greater than the maximum delay tolerance T, then $\hat{A}_{k-1}(1)-1-T+L_{k-1}$ cells will be dropped. In general, the number of cells that must be discarded by time $t^g_{k-1}+\tau$, namely $\hat{d}_k(\tau)$, is given by

$$\begin{aligned}\hat{d}_k(\tau) &= \max\left\{0, \max_{1\le\tau'\le\tau}[\hat{A}_{k-1}(\tau')-(\tau'+T-L_{k-1})]\right\}\\ &= \max\left\{0, \max_{1\le\tau'\le\tau}[\hat{A}_{k-1}(\tau')-f_{\tau'}]\right\}\end{aligned}$$

where $f_{\tau'}=\tau'+T-L_{k-1}$, $0\le\tau'\le L_{k-1}$. An example of the evolution of the process $\{\hat{A}_{k-1}(\tau)\}_{\tau=0}^{L_{k-1}}$ and the linear function f_τ is shown in Fig. 3. Notice that f_τ represents the maximum number of arrivals up to time τ which can be transmitted before their deadline expires. It should also be noted that cells may be dropped even if the total number of arrivals over the $(k-1)$th service cycle is less than or equal to T. In fact, the number of cells which are dropped (will not meet their deadline) is determined by the maximum difference between $\{\hat{A}_{k-1}(\tau)\}_{\tau=0}^{L_{k-1}}$ and f_τ, as indicated in the above equation.

Let $\hat{m}_k(\tau)=\max_{1\le\tau'\le\tau}[\hat{A}_{k-1}(\tau')-\tau']$. Then $\hat{d}_k(\tau)$ can be rewritten as $\hat{d}_k(\tau)=\max\{0,\hat{m}_k(\tau)-(T-L_{k-1})\}$. Notice that $\hat{d}_{r,k}$—the total number of cells dropped at t_k, that is at the beginning of the kth service cycle—will be equal to $\hat{d}_k(L_{k-1})$.

Let $A_j(\tau)$, $m(\tau)$, $d_j(\tau)$, and $d_{r,j}$ with $j=L_{k-1}$ be the random variables associated with $\hat{A}_{k-1}(\tau)$, $\hat{m}_k(\tau)$, $\hat{d}_k(\tau)$, and $\hat{d}_{r,k}$, respectively. These random variables do not depend on the time t^g_k but only on the previous cycle's length L_{k-1} described by j.

Notice that $\{A_j(\tau)\}_{\tau=0}^{j}$ represents a right-continuous, discrete-valued, cumulative arrival process which has initial value zero ($A_j(0)=0$), evolves for j time slots, and has independent increments. The probability of μ arrivals at any given discrete-time (increment) is given by l_μ. For $j=L_{k-1}$, by definition

$$\begin{aligned}&m(\tau)=\max_{1\le\tau'\le\tau}[A_j(\tau')-\tau'],\\ &d_j(\tau)=\max\{0,m(\tau)-(T-j)\},\qquad d_{r,j}=d_j(j).\end{aligned}$$

Notice that $d_{r,j}$ denotes the number of cells dropped at the beginning of a service cycle that follows a service cycle of length j; its probability is given by

$$\begin{aligned}P\{d_{r,j}=d\} &= P\{d_j(j)=d\}\\ &= \begin{cases}P\{m(j)=T-j+d\}, & \text{if } d\ge 1\\ P\{m(j)\le T-j\}, & \text{if } d=0.\end{cases}\end{aligned}$$

$P_j(\epsilon)$ is defined by

$$P_j(\epsilon)=\begin{cases}P\{m(j)=\epsilon\}, & \text{if } \epsilon\ge 1\\ P\{m(j)\le 0\}, & \text{if } \epsilon=0\\ 0, & \text{elsewhere}\end{cases}$$

and a recurrent expression for its computation is presented in Appendix II.

Thus, the conditional expected number of dropped cells at the present frame given the previous frame length is L $(\overline{d}^I_{r/L}(T))$ is given by

$$\begin{aligned}\overline{d}^I_{r/L}(T) &= E\left\{\hat{d}_{r,k}/L_{k-1}=L\right\}\\ &= \sum_{d=1}^{+\infty} dP\left\{\hat{d}_{r,k}=d/L_{k-1}=L\right\}\\ &= \sum_{d=1}^{+\infty} dP\{d_{r,L}=d\}\\ &= \sum_{d=1}^{+\infty} dP\{m(L)=T-L+d\}\\ &= \sum_{d=1}^{+\infty} dP_L(T-L+d).\end{aligned}$$

From the above expression, the conditional expected number of dropped cells for all values of L $(1\le L\le T)$ may be computed requiring a computational complexity of $O(\frac{1}{2}n^2T^2)$. This complexity may be further simplified if (11) in Appendix II is applied in the above equation. After necessary simplifications, the following recurrent formula is obtained:

$$\begin{aligned}\overline{d}^I_{r/L}(T) &= \overline{d}^I_{r/L-1}(T)+\lambda G_{L-1}(T)\\ &\quad+\sum_{\mu=0}^{n-1}\sigma_\mu P_{L-1}(T-(L-1)-\mu)\end{aligned}\tag{3}$$

$$G_L(T)=G_{L-1}(T)+\sum_{\mu=0}^{n-1}\omega_\mu P_{L-1}(T-(L-1)-\mu)\tag{4}$$

$$P_L(\epsilon)=\begin{cases}\displaystyle\sum_{\mu=0}^{\min\{n,\epsilon+1\}} l_\mu P_{L-1}(\epsilon+1-\mu), & \text{if } \epsilon\ge 1\\ l_0P_{L-1}(0)+l_0P_{L-1}(1) & \\ \quad +l_1P_{L-1}(0), & \text{if } \epsilon=0\\ 0, & \text{elsewhere.}\end{cases}\tag{5}$$

With initial conditions $\overline{d}^I_{r/0}(T)=G_0(T)=0$, and $P_0(\epsilon)=\delta(\epsilon)$ [i.e., zero always except at $P_0(0)=1$], σ_μ was already defined as $\sigma_\mu=\sum_{j=1}^{n-\mu} jl_{\mu+j}$ in Appendix I-C.[1] $\omega_\mu=\sum_{j=1}^{n-\mu} l_{\mu+j}$ is the probability that more than μ cells arrive at any given time slot. $G_L(T)$ may be interpreted as the probability that there is a cell dropped at the present service cycle given that the previous frame length was L and the maximum delay tolerance is T. Numerically $G_L(T)=\sum_{j=T-L+1}^{+\infty}P_L(j)$ and will always be lower than one.

It should be noted that since $P_j(\epsilon)=0$ if $\epsilon<0$, the summations in the above equation need to be evaluated only for $\min\{T-(L-1),n-1\}$ terms. Also, there is no need to compute $P_L(\epsilon)$ for values of $\epsilon>T-L$. Thus, using the above recurrent expression, computing the conditional expected number of dropped cells for all values of $L(1\le L\le T)$ requires a complexity of $O(\frac{1}{2}nT^2-\frac{1}{2}n^2T+\frac{1}{6}n^3)$ when $T\gg n$. It is clear that the complexity has been reduced by an order of magnitude. Even better, when $n>T$ the

[1] Strictly speaking σ_0 has not been defined before. It should be noted that $\sigma_0=\lambda$.

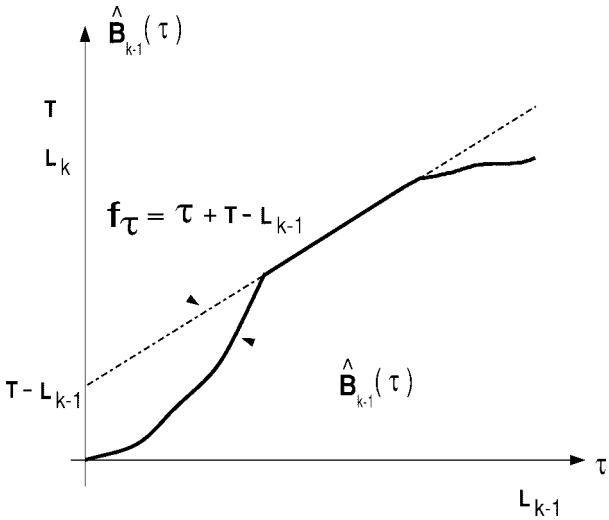

Fig. 4. Number of "surviving" cells $\hat{B}_{k-1}(\tau)$ among the cells arrived up to time $t^g_{k-1} + \tau$.

complexity is limited to be $O(\frac{1}{6}T^3)$. This allow us to compute the dropping rate even for the case of n equal to infinity.

B. Service Cycle Length's Probability Distribution, $P^I_{ij}(T)$

The kth cycle length is given by

$$L_k = \hat{A}_{k-1}(L_{k-1}) - \hat{d}_k(L_{k-1})$$

and since $\hat{A}_{k-1}(L_{k-1})$ and $\hat{d}_k(L_{k-1})$ are correlated, it is not easy to compute $P^I_{ij} = P\{L_k = i/L_{k-1} = j\}$ from the above equation. The process $\{\hat{B}_{k-1}(\tau)\}_{\tau=0}^{L_{k-1}}$ with generic representation $\{B_j(\tau)\}_{\tau=0}^{j}$ (with $j = L_{k-1}$) will be considered. $\hat{B}_{k-1}(\tau)$ represents the number of "surviving" (i.e., neither dropped nor assigned for transmission yet) cells among the cells arrived up to time $t^g_{k-1}+\tau$. Thus, for the variable frame length case

$$\hat{B}_{k-1}(\tau) = \hat{A}_{k-1}(\tau) - \hat{d}_k(\tau) \quad \text{and} \quad B_j(\tau) = A_j(\tau) - d_j(\tau).$$

An example of the evolution of $\{\hat{B}_{k-1}(\tau)\}_{\tau=0}^{L_{k-1}}$ is shown in Fig. 4. This evolution can be interpreted as if the cells that will have to be dropped, are being discarded as soon as this is realized, that is, each time $B_{k-1}(\tau)$ tends to become greater than the line $f_\tau = T - L_{k-1} + \tau$. It follows that

$$\begin{aligned} L_k &= \hat{B}_{k-1}(L_{k-1}) \\ P^I_{ij} &= P\{L_k = i/L_{k-1} = j\} \\ &= \begin{cases} P\{\hat{B}_{k-1}(L_{k-1}) = i/L_{k-1} = j\}, & \text{if } i \geq 2 \\ P\{\hat{B}_{k-1}(L_{k-1}) = 1 \text{ or } 0/L_{k-1} = j\}, & \text{if } i = 1 \end{cases} \\ &= \begin{cases} P\{B_j(j) = i\}, & \text{if } i \geq 2 \\ P\{B_j(j) = 1\} + P\{B_j(j) = 0\}, & \text{if } i = 1. \end{cases} \end{aligned}$$

Let $PB^j_\tau(i, T) = P\{B_j(\tau) = i/\text{maximum delay tolerance} = T\}$, then the following recurrent formulas holds:

$$PB^j_\tau(i, T) = \begin{cases} \sum_{\mu=0}^{n} l_\mu PB^j_{\tau-1}(i-\mu, T), & \text{if } i < T - j + \tau \\ \sum_{\mu=1}^{n} \left(\sum_{\epsilon=\mu}^{n} l_\epsilon \right) PB^j_{\tau-1}(i-\mu, T), & \text{if } i = T - j + \tau \end{cases}$$

with the initial conditions

$$PB^j_0(i, T) = \begin{cases} 1, & \text{if } i = 0 \\ 0, & \text{elsewhere.} \end{cases}$$

The first equation holds since no cell is dropped in the actual time slot (τ) when $i < T-j+\tau$; thus, $B_j(\tau) = B_j(\tau-1)+a_\tau$, where a_τ is the number of cells arriving at time τ (as before $l_\mu = P\{a_\tau = \mu\}$). The second equation holds since cells may be dropped when $i = T-j+\tau$. Thus, given that $B_j(\tau-1) = x$, then if (and only if) $a_\tau \geq T-j+\tau-x$ then $B_j(\tau) = T-j+\tau$.

From the above recurrent equations P^I_{ij} may be calculated as

$$P^I_{ij} = \begin{cases} PB^j_j(i, T), & \text{if } i \geq 2 \\ PB^j_j(1, T) + PB^j_j(0, T), & \text{if } i = 1 \end{cases}$$

and then the steady-state probability distribution of the service cycle length $\prod^I_i = P\{L_k = i\}$ can be computed.

Finally, the dropping rate $d^I_r(T)$ is computed from $\overline{d}^I_{r/L}(T)$ and $\prod^I_i$ by using (2).

IV. The Real Variable Frame Length TDMA (RVFL-TDMA) Scheme

The RVFL-TDMA scheme is analyzed in this section [see Fig. 2(b)]. The only difference between this scheme and the previous one (Section III) is the consideration of the frame overhead. In this real scheme, the first Re time slots at the beginning of every service cycle are consumed by the user's transmission requests; these Re time slots are referred to as the reservation period. The next In time slots are used by the scheduler to inform the users of its decisions (slot assignments) and are referred to as the information period. It is assumed that both Re and In are fixed and independent of the traffic load.

The kth service cycle begins at time $t^g_k - Re$, when the scheduler begins to receive the previous service cycle's arrival information of each user. At time t^g_k the scheduler has all the required information, takes its scheduling decision and informs the users during the next In time slots. At time $t^g_k + In$ the user's data transmissions (receptions) begin.

Let $t^g_{k,j}$ denote the time at which the jth user completes the transmission of its request for slots of the kth frame, that is, provides to the scheduler information regarding its arrivals over the $(k-1)$th frame; $t^g_k - Re \leq t^g_{k,j} \leq t^g_k$. Clearly, this request will be based on user information (to be transmitted) which is generated before $t^g_{k,j}$. By assuming that this request (at $t^g_{k,j}$) represents all the information generated by user j until t^g_k or $t^g_k - Re$, the auxiliary systems L and U are constructed.

That is, the following key assumptions are made regarding the content of the requests from all users, leading to systems L and U:

- L at time t_k^g the scheduler knows about all arrivals up to time t_k^g;
- U at time t_k^g the scheduler knows only about the arrivals up to time $t_k^g - Re$.

Under the auxiliary system L, a cell arriving over the interval $\langle t_{k,j}^g, t_k^g\rangle$ will be considered for service during the kth service cycle. Under the real scheme this cell will be considered for service in the $(k+1)$th service cycle. Clearly, the cell delay under the real scheme will be shaped by an additional service cycle length ($Re + In +$ data) compared to that under system L. Thus, the auxiliary system L outperforms the real system. A similar argument between the real system and auxiliary system U regarding cells generated over $\langle t_k^g - Re, t_{k,j}^g\rangle$ establishes that the real scheme outperforms the auxiliary system U.

Let the superscripts I, R, L, U indicate a quantity associated with the IVFL-TDMA scheme, RVFL-TDMA scheme, auxiliary system L and auxiliary system U, respectively. In view of the above discussion it is easy to establish that $d_r^I < d_r^L \leq d_r^R \leq d_r^U$.

The auxiliary systems L and U will be studied to calculate tight (as it will be shown) bounds on the performance induced by the real, variable frame length, gated scheme.

A. Dropping Rate Induced by the Auxiliary System L, $d_r^L(T)$

Since the maximum delay tolerance is T, the service of the last cell served over the kth service cycle must be completed by $t_k^g + T$. Thus, the maximum length of a busy (at least one served) frame will be equal to $t_k^g + T - (t_k^g - Re)$. Due to the overhead, the length of an empty frame will be equal to $Re + In$. Thus $Re + In \leq L_k \leq Re + T$ for any k.

Let $\hat{A}_{k-1}(\tau)$, for $0 \leq \tau \leq L_{k-1}$, represent the number of cell arrivals (generations) over τ consecutive slots following t_{k-1}^g (as before, Section III); such arrivals will be considered for service during the kth frame [see Fig. 2(b)]. Clearly, $\hat{A}_{k-1}(L_{k-1})$ represents all the arrivals (between t_{k-1}^g and t_k^g) to be considered for service during the kth frame.

Since $\hat{A}_{k-1}(\tau)$ cells have arrived at time $t_{k-1}^g + \tau$, then the last of these cells will have to wait $L_{k-1} - Re - \tau$ time slots [the remaining time for the end of the $(k-1)$th service cycle] plus the overhead period ($Re + In$ time slots) plus $\hat{A}_{k-1}(\tau)$ time slots, in order to complete its transmission. Clearly, if this time $(\hat{A}_{k-1}(\tau) - \tau + L_{k-1} + In)$ is greater that T time slots some cells will be dropped. Thus, the number of cells arrived over $\langle t_{k-1}^g, t_{k-1}^g + \tau\rangle$ which must be discarded is given by

$$\begin{aligned}\hat{d}_k^L(\tau) &= \max\left\{0, \max_{1\leq\tau'\leq\tau}[\hat{A}_{k-1}(\tau) - (\tau + T - In - L_{k-1})]\right\}\\ &= \max\left\{0, \max_{1\leq\tau'\leq\tau}[\hat{A}_{k-1}(\tau) - (\tau + T' - L_{k-1})]\right\}\end{aligned}$$

where $T' = T - In$. For $L_{k-1} \leq T'$ this expression is the same to the one obtained in Section III-A. The results of Section III for the conditional dropping rate and the frame length are still valid here.

Let $\overline{d}_{r/j}^I(T)$ be the conditional expected number of dropped cells in the present frame given that the previous frame length was j, for the IVFL-TDMA scheme with maximum delay tolerance equal to T time slots, as computed in Section III-A; let $PB_\tau^j(i, T)$ be the probability that i cells survived among those arrived over τ consecutive slots following the time by which all past arrivals had already been considered, given that the maximum number of surviving cells up to this time is equal to $\tau + T - j$ as computed in Section III-B. Two cases need to be considered.

Case 1: $Re + In \leq j = L_{k-1} \leq T' = T - In$. Processes $\hat{A}_{k-1}(\tau)$ and $\hat{B}_{k-1}(\tau)$ (defined in Section III-B) evolve as processes $A_j(\tau)$ and $B_j(\tau)$ with maximum delay tolerance $T' = T - In$, respectively. Taking into consideration that $L_k = \hat{B}_{k-1}(L_{k-1}) + Re + In$ the following "adjustments" to the quantities derived in Section III lead to the corresponding quantities associated with the auxiliary system L

$$\overline{d}_{r/j}^L(T) = \overline{d}_{r/j}^I(T - In)$$

and

$$P_{ij}^L = PB_j^j(i - Re - In, T - In) \tag{6}$$

where $\overline{d}_{r/j}^L(T)$ and P_{ij}^L denote the conditional expected number of dropped cells in the present frame given that the length of the previous frame is j, and the probability that the present frame length is i given that the previous frame length is j, respectively.

Case 2: $T' = T - In < j = L_{k-1} \leq Re + T$. The cells arriving at the first $j - T'$ time slots of frame $(k-1)$th will be discarded; for the remaining T' time slots, $\hat{A}_{k-1}(\tau')$ and $\hat{B}_{k-1}(\tau')$ will evolve as processes $A_j(\tau')$ and $B_j(\tau')$ with maximum delay tolerance T' and length $j' = T'$. Then

$$\overline{d}_{r/j}^L(T) = (j - T + In)\lambda + \overline{d}_{r/T-In}^I(T - In)$$

and

$$P_{ij}^L = PB_{T-In}^{T-In}(i - Re - In, T - In) \tag{7}$$

where λ denotes the mean number of arrivals per slot.

Finally

$$d_r^L(T) = \frac{\displaystyle\sum_{j=Re+In}^{Re+T} \prod_j^L \overline{d}_{r/j}^L(T)}{\displaystyle\sum_{j=R+I}^{R+T} j \prod_j^L} \tag{8}$$

where $\prod_i^L = P\{L_k = i \text{ at system } L\}$ and it is computed from P_{ij}^L.

Additionally, an alternative expression to compute the dropping rate is presented in Appendix IV. Equation (13) does not require the computation of $\overline{d}_{r/j}^L(T)$ but on the other hand it is numerically unreliable. It is presented mainly to help in the qualitative analysis of the RVFL-TDMA scheme (at the conclusion).

B. Dropping Rate Induced by the Auxiliary System U, $d_r^U(T)$

In the auxiliary system L, arrivals over the overhead period $Re + In$ are treated differently. The arrivals over Re are served in the immediate service cycle while arrivals over In are served one service cycle later. In the auxiliary system U all arrivals over $Re + In$ are served later. Thus, the auxiliary system U can be viewed as equivalent to an auxiliary system L with parameters $Re' = 0$ and $In' = Re + In$. It is easy to establish that the performance of system U can be derived from the performance of the corresponding L system with delay tolerance reduced by Re. That is, $Re' = Re$, $In' = In$, and $T' = T - R$ and finally

$$d_r^U(T) = d_r^L(T - Re).$$

V. The Real Fixed Frame Length TDMA (RFFL-TDMA) Scheme

Consider the RVFL-TDMA scheme in which the frame length L_k is not variable (on-demand) but fixed and equal to L_f time slots. As before, two auxiliary systems are defined.

- FL At time t_k^g the scheduler knows about all arrivals up to time t_k^g.
- FU At time t_k^g the scheduler knows only about the arrivals up to time $t_k^g - Re$.

Let the superscripts FL, FR, and FU indicate a quantity associated with the auxiliary system FL, RFFL-TDMA scheme, and auxiliary system FU, respectively. Similarly to Section IV, it is easy to establish that $d_r^{FL} \leq d_r^{FR} \leq d_r^{FU}$.

The auxiliary systems FL and FU will be studied to calculate tight bounds on the performance induced by the RFFL-TDMA scheme.

A. Dropping Rate Induced by the Auxiliary System FL, $d_r^{FL}(T)$

An approach similar to the one used before to compute the dropping rate of the IVFL-TDMA scheme is employed here. The complete procedure is explained in Appendix III.

B. Dropping Rate Induced by the Auxiliary System FU, $d_r^{FU}(T)$

Using an argument similar to the one used in Section IV-B, it can be claimed that the system FU can be viewed as equivalent to an auxiliary system FL with parameters $Re' = 0$ and $In' = Re + In$. Thus, it is easy to establish that the performance of system FU can be derived from the performance of the corresponding FL system with delay tolerance reduced by Re. That is $Re' = Re$, $In' = In$, and $T' = T - R$ and finally

$$d_r^{FU}(T) = d_r^{FL}(T - Re).$$

VI. Numerical Results and Discussion

In this section the performance of the various TDMA schemes presented in this paper is investigated by employing the analytical studies presented in the previous sections. In addition to evaluating the impact of the key parameters—such as the maximum delay tolerance T, the number of applications N, the length of frame overhead, etc.—some of the results point to the performance advantage of certain schemes over others.

The lower and upper bounds on the dropping rate induced under a RVFL-TDMA scheme supporting $N = 6$ Bernoulli users are calculated by employing the auxiliary systems L and U and using the expressions derived in Section IV; the per user traffic rate is equal to 0.15. The results are presented in Fig. 5 as a function of the maximum delay tolerance T and for various values of (Re, In). For the (small) values of the frame overhead $(Re + In)$ considered turns out that the bounds are very tight, suggesting that the results under the auxiliary system L (lower bound) can serve as a good approximation on the exact dropping rate. The results suggest that a small increase in the length of the frame overhead results in a significant increase in the dropping rate. Thus it may be worth trying to reduce the length of the frame overhead by employing mechanisms such as piggy-backing and arrival time estimation.

Fig. 6 depicts the lower bound on the dropping rate under the RVFL-TDMA scheme under different traffic configurations. The results are shown as a function of T and for various values of $(Re, In) = (ov, 0)$— ov is short for overhead. Fig. 6(a) is derived for a set of $N = 6$ Bernoulli users with per user rate of 0.15 (total rate $\lambda = 0.9$); Fig. 6(b) is derived for a set of $N = 5$ Bernoulli users with per user rate of 0.20 ($\lambda = 1.0$); Fig. 6(c) is derived for a set of $N = 4$ Bernoulli users with per user rate of 0.20 ($\lambda = 0.8$); Fig. 6(d) is derived for a set of $N = 50$ Bernoulli users with per user rate of 0.016 ($\lambda = 0.8$).

From the values in Fig. 6 (in log scale) the exponential decay of the dropping rate can be observed for large T. This is the case not only under zero frame overhead (as expected from Section II) but also in the presence of frame overhead. By considering the results in Fig. 6(c)–(d) for small frame overhead length it can be concluded that the induced dropping rate for $N = 50$ users [Fig. 6(d)] is significantly greater than that for $N = 4$ users [Fig. 6(c)], although $\lambda = 0.8$ in both cases. This difference may be attributed to the larger variance of the traffic for $N = 50$ and decreases as the frame overhead increases. Thus, the variance and burstiness of the traffic in addition to the rate may impact significantly on the induced dropping rate.

The maximum number of users that can be supported under the RVFL-TDMA scheme can be determined by considering the results in Fig. 7, presenting the dropping rate as a function of the number N of supported Bernoulli users and for various values of $(Re, In) = (overhead, 0)$; note that for a given (frame) overhead length, setting $Re = overhead$ and $In = 0$ will yield the lowest dropping rate for the particular TDMA scheme. The results shown in Fig. 7 quantify the (negative) impact of the frame overhead on the system utilization when a certain level of QoS (dropping rate) is to be delivered; the per user rate is 0.01 and the maximum delay tolerance is 100 time slots.

If a specific cell loss probability (as opposed to system dropping rate) is desired, then the cell loss probability can

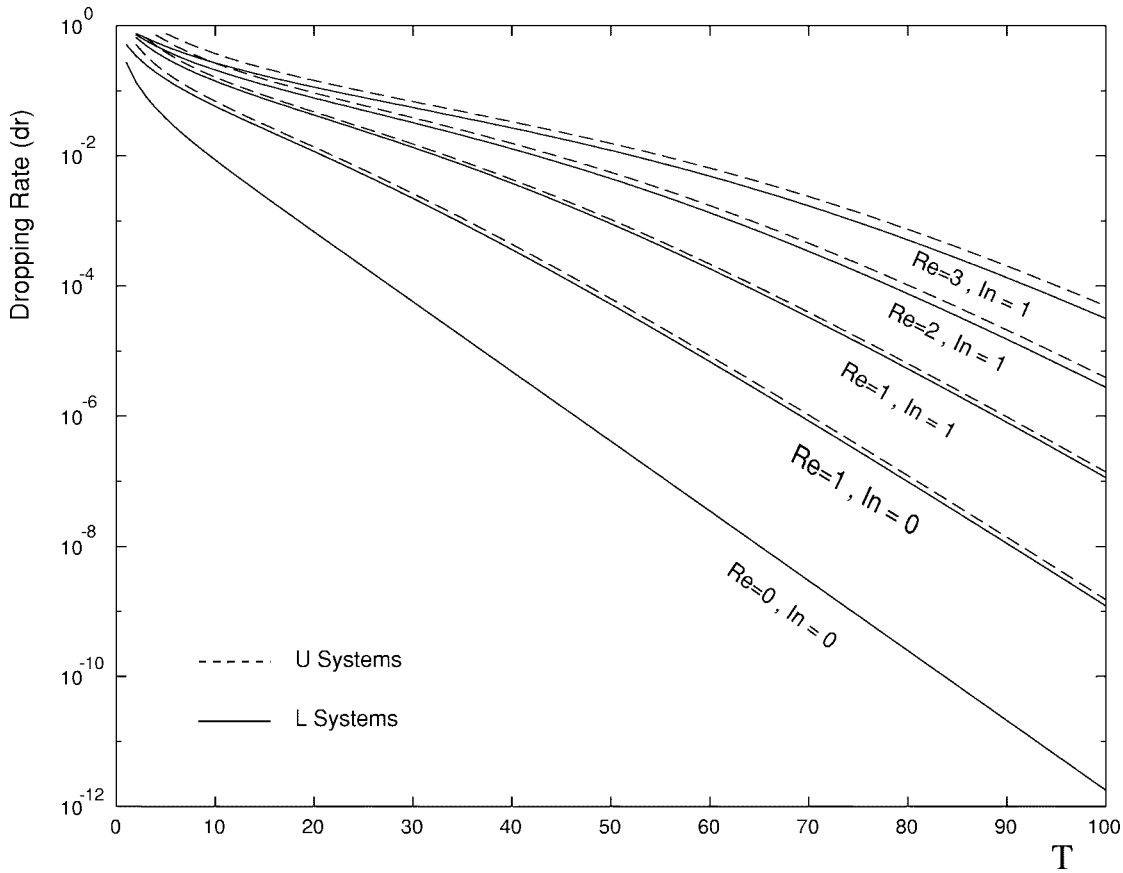

Fig. 5. Dropping rate bounds under the RVFL-TDMA scheme versus maximum delay tolerance (T) for various values of (Re, In); total traffic rate is $\lambda = 0.9$.

be derived as the ration of the system dropping rate and total arrival rate ($\lambda = 0.01N$). For example, for a maximum cell loss probability of 10^{-12}, reducing the frame overhead length from four to zero will allow to increase the number of supported users from $N \approx 78$ to $N \approx 87$, an increase of approximately equal to 11.5%.

The (system) dropping rate under the RFFL-TDMA scheme is shown in Fig. 8 as a function of the (fixed) frame length L_f; the frame overhead is given by $(Re = 2, In = 0)$ and $T = 100$. In Fig. 8(a) is obtained for $N = 4$ ($\lambda = 0.8$) and and (b) for $N = 5$ ($\lambda = 1.0$) users, respectively; the per Bernoulli user rate is 0.2. Since the bounds on the dropping rate derived from the auxiliary systems FL and FU (Section V) are very tight, and only the lower bound is plotted. It can be observed that for a given set of supported applications there exists an optimal (fixed) frame length (namely L_f^*) minimizing the induced dropping rate. This optimal frame length is, in general, different for a different set of supported applications, as illustrated in Fig. 8. It should be noted that all results under the RFFL-TDMA scheme presented below are obtained for the optimal value of the (fixed) frame length L_f^*.

The dropping rate under the RFFL-TDMA scheme employing the optimal frame length L_f^* is plotted in Fig. 9 as a function of T and the values of the frame overhead $(Re, In) = (1, 0)$ and $(Re, In) = (2, 0)$. The results are shown in Fig. 9(a) for $N = 4$ ($\lambda = 0.8$) and and (b) for $N = 5$ ($\lambda = 1.0$) Bernoulli users, respectively. Note that the case of zero frame overhead is not considered since in this case $L_f^* = 1$ and the resulting TDMA scheme becomes equivalent to the ICE-TDMA scheme.

Results from Figs. 6 and 9 are plotted together in Fig. 10 to illustrate the improved performance induced by a variable frame (RVFL-TDMA) scheme compared to that of a fixed frame (RFFL-TDMA) scheme. Fig. 11 shows the dropping rate as a function of the number of users under both the RVFL-TDMA scheme (results also shown in Fig. 7) and the RFFL-TDMA scheme. This figure illustrates the (positive) impact that allowing the frame length to vary on demand (instead of being fixed) has on the maximum number of admitted users, when a certain level of QoS is to be delivered. As before (Fig. 7), the users are Bernoulli with a per user rate of 0.01, the maximum delay tolerance is 100 time slots, and $(Re, In) = (overhead, 0)$ (with $overhead = 1, 2, 3$). It can be noted that the gap between the schemes increases if the frame overhead length is increased or the required dropping rate is reduced (higher quality of service). When it is required to deliver a dropping rate of at most 10^{-16}, using the RVFL-TDMA scheme instead of the RFFL-TDMA scheme (for the same overhead) will increase the number of admitted users by up to a 10%. This gain decreases when the induced dropping rate is allowed to increase. When the required dropping rate is around 10^{-4} the difference in the number of admitted users under both schemes will be around 3%. These figures (Figs. 10 and 11) quantify an important result of this paper.

The relative performance of various TDMA schemes is shown in Fig. 12 under various traffic environments: $N = 6$

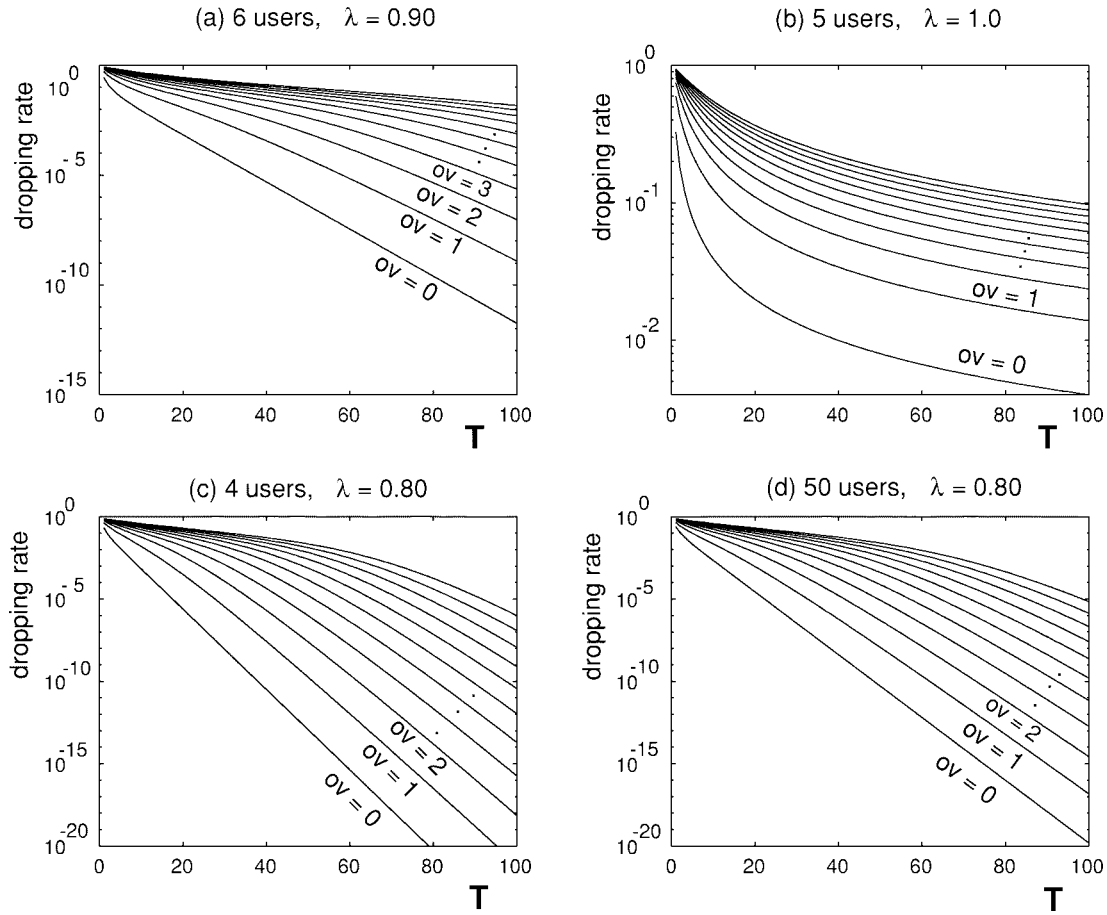

Fig. 6. Dropping rate versus maximum delay tolerance (T) for different configurations of the RVFL-TDMA scheme.

Bernoulli users each of rate 0.15 ($\lambda = 0.9$) are considered in case (a) and $N = 5$ Bernoulli users each of rate 0.20 ($\lambda = 1.0$) are considered in case (b). $N = 8$ ($N = 10$) bursty users with total rate of $\lambda = 0.8$ ($\lambda = 1.0$) are considered in case (c) [case (d)]. A bursty user generates zero or ten cells per slot with corresponding probabilities 0.99 and 0.01, resulting in a rate of 0.1 cells/slot. Results are presented under the FF-TDMA scheme with $L_f = N$, the IVFL-TDMA (or ICE-TDMA) scheme and various RVFL$_k$-TDMA schemes, where k represents the total overhead. The IVFL-TDMA scheme is the RVFL$_k$-TDMA scheme with $k = 0$ (no overhead).

The FF-TDMA scheme with $L_f = N$ models a TDMA scheme which allocates one slot to each user; no overhead is present since no communication between the users and the scheduler is necessary (similar to the TDM scheme used in the T-1 system for voice transmission). The results under this FF-TDMA scheme can be obtained by calculating the dropping rate for each user from the study of an FL system with parameters $L_f = N$, $Re = N-1$, and $In = 0$ and adding the results for all users. That is, each user may be viewed as being alone in a RFFL-TDMA scheme with overhead $Re = N - 1$, $In = 0$.

The IVFL-TDMA (ICE-TDMA) scheme—RVFL$_k$-TDMA scheme with $k = 0$—is the optimal scheme yielding the minimum possible system dropping rate. No slots are wasted under the IVFL-TDMA (ICE-TDMA) scheme (no preallocation of slots) while user/scheduler information exchange is assumed without any overhead ($k = 0$).

The RVFL$_N$-TDMA scheme (i.e., $k = N$) considered in this figure assumes a contention-free request reservation scheme which utilizes $Re = N$ full slots per frame. That is, each user has its own full slot for reservations; $In = 0$. Typically, it is expected that minislots (as opposed to slots) would be assigned to users for reservations yielding to a much smaller value of Re. The results under RVFL$_k$-TDMA schemes are obtained by employing the auxiliary system L analyzed in Section IV.

The results shown in Fig. 12 demonstrate behavior anticipated from the insight and discussions presented in this paper. No scheme outperforms the IVFL-TDMA (ICE-TDMA) scheme under any system configuration. Under bursty traffic the FF-TDMA scheme is the poorest under all values of λ and T considered. Under the (less bursty, or more regular) Bernoulli traffic and rate $\lambda = 1$ the FF-TDMA scheme outperforms some of the RVFL$_k$-TDMA schemes (for $k \geq 2$), while for lower rates ($\lambda = 0.9$) the FF-TDMA scheme is outperformed by the RVFL$_k$-TDMA scheme for small k and/or large values of T.

VII. Conclusions and Comments

A closed-form expression was developed for the lower bound for the induced system dropping rate in a multiaccess TDMA network supporting users with a common maximum

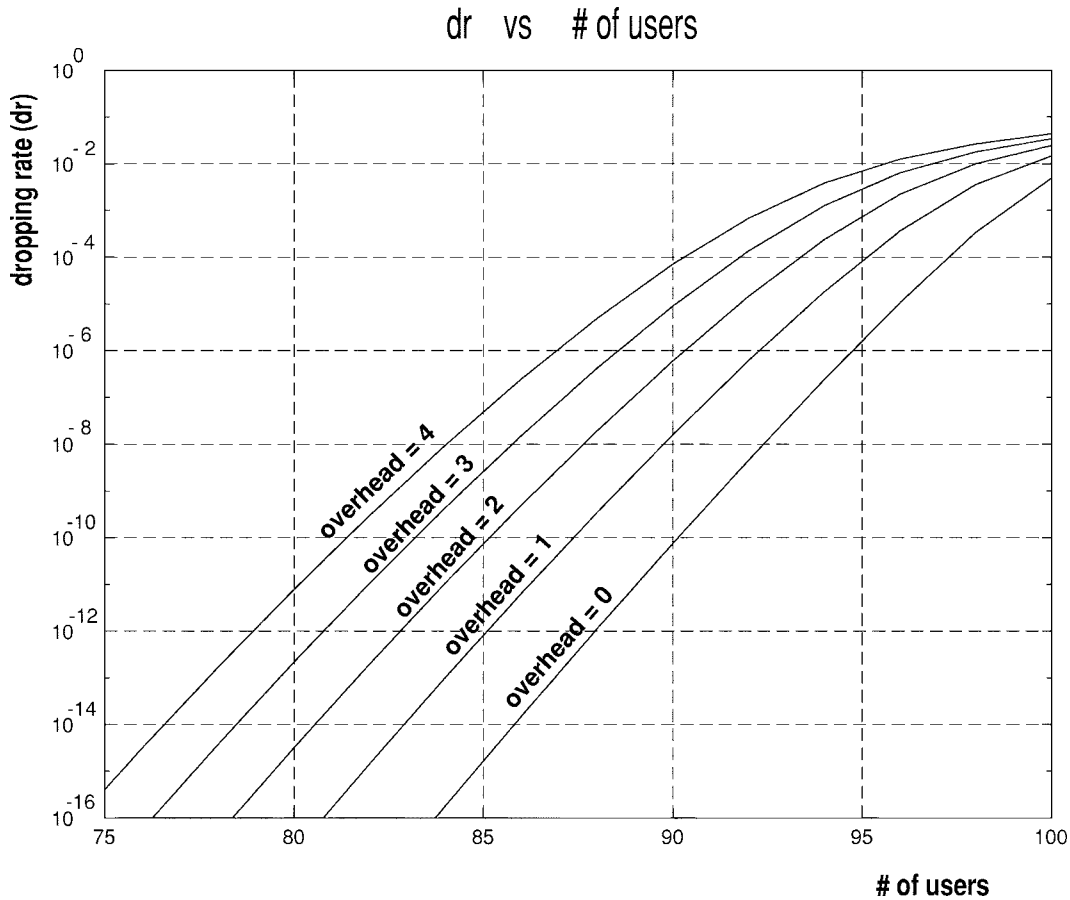

Fig. 7. Dropping rate versus number of users for the RVFL-TDMA scheme; maximum delay tolerance $T = 100$ time slots.

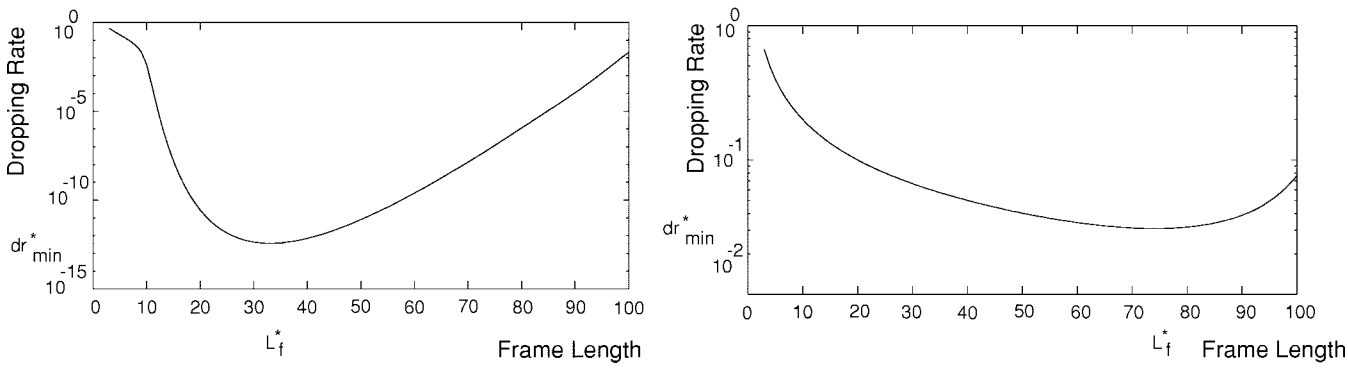

Fig. 8. Dropping rate versus frame length (fixed) for the RFFL-TDMA scheme; maximum delay tolerance $T = 100$ time slots. (a) $\lambda = 0.8$, total overhead $= 2$ and (b) $\lambda = 1.0$, total overhead $= 2$.

delay tolerance. This lower bound (result obtained for the ICE-TDMA and IVFL-TDMA schemes) depends only on the traffic characteristics.

It may be observed that for arrival rates lower than one, the dropping rate is an inversely linear function of the maximum delay tolerance T for small values of T ($T < 1/(1-r_d)$) and it is approximately exponential for large values of T [$T > 1/(1-r_d) = N(r_d)/(1-\lambda)$].[2] For such arrival rates, the dropping rate depends not only on the first two moments (mean arrival rate and its variance) but also on the particular "shape" of the arrival process [i.e., function $D(z)$]. For arrival rates closer to one, the inversely linear region is larger. In the limiting case ($\lambda = 1$), the inversely linear behavior dominates for all values of T. Also, for arrival rates close to one the dependency on the particular "shape" of the arrival process [i.e., $D(z)$] is smaller. When the arrival rate equals one, the dropping rate function basically depends on the mean arrival rate (λ), the variance (σ_l^2), and the inverse of the maximum delay tolerance ($1/T$). This may be explained since in this case the different states in the queue are almost equiprobable, and cells will be dropped only if the queue is close to full which happens with

[2] See Appendix I-C.

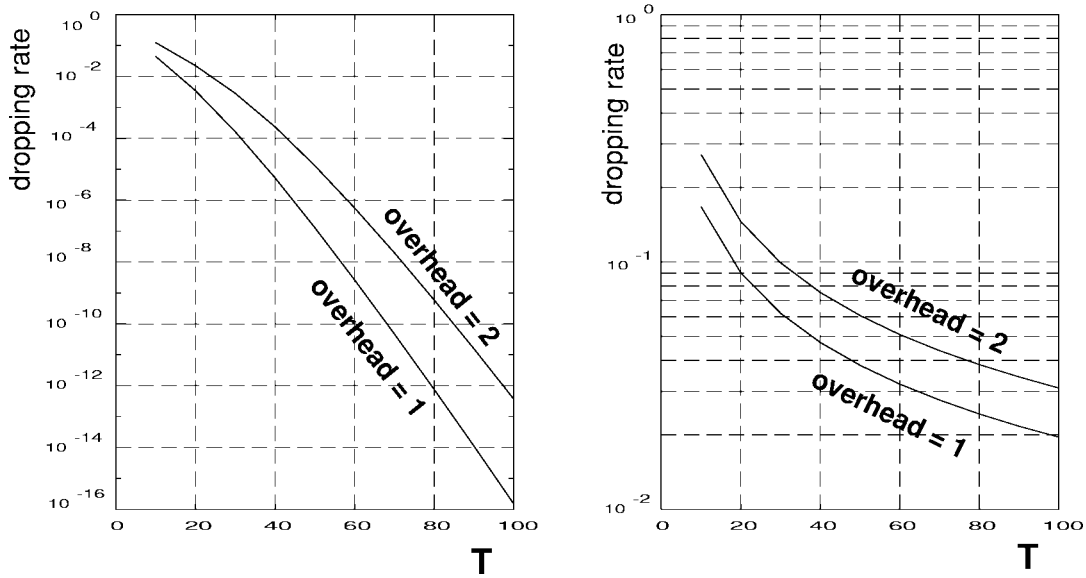

Fig. 9. Dropping rate versus maximum delay tolerance (T) for the RFFL-TDMA scheme. (a) Four users, $\lambda = 0.8$ and (b) five users, $\lambda = 1.0$.

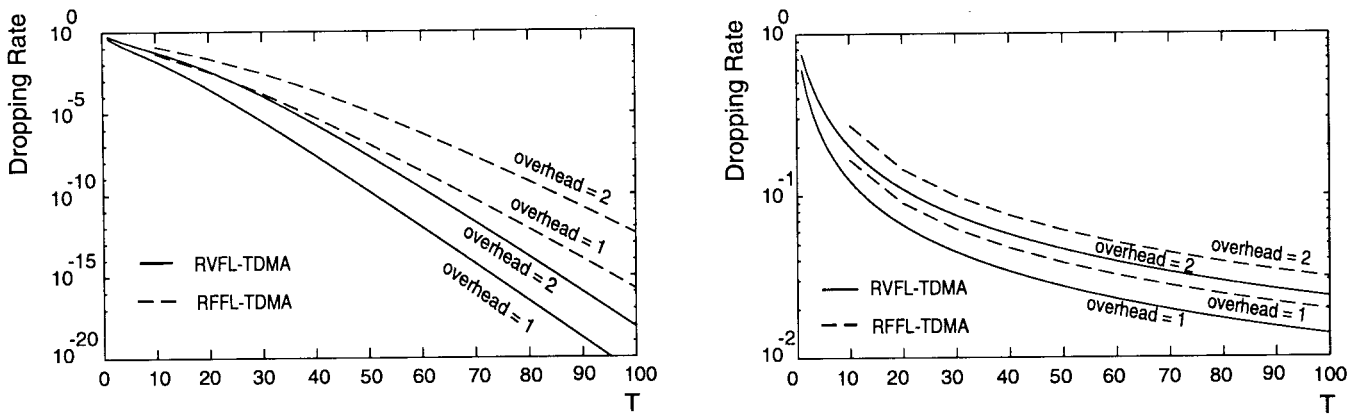

Fig. 10. Dropping rate under RVFL-TDMA and RFFL-TDMA schemes versus maximum delay tolerance (T). (a) Four users, $\lambda = 0.8$ and (b) five users, $\lambda = 1.0$.

probability inversely proportional to the number of states (in this case equal to T). For arrival rates greater than one (not of interest) and moderate values of T, the dropping rate function is approximately equal to a constant value equal to the excess of the arrival rate over one (i.e., it is only dependent on the arrival rate, not even on T). The latter behavior may be explained since for arrival rates greater than one the system will tend to be full (in the long range). A system full may only accept one new cell each time slot. Therefore the remaining $\lambda - 1$ cells will have to be dropped. It may be seen that even if the maximum delay tolerance is increased, the system will eventually become full and the dropping rate will be practically unaffected.

Expressions were developed for various schemes that can be implemented in a TDMA network (IVFL-TDMA, RVFL-TDMA, and FF-TDMA) for the computation of tight bounds on the induced system dropping rate in each case.

For the RVFL-TDMA scheme, it was found that for moderate arrival rates (less than 1 cell/slot) a small increase in the frame overhead length will affect the achievable dropping rate by several orders of magnitude. Thus, more effort should be put toward reducing this overhead length.

For arrival rates lower than one and for nonzero overhead (under the RVFL-TDMA scheme) the dropping rate as a function of the maximum delay tolerance exhibits a similar behavior as in the case of the ICE-TDMA scheme; that is, for small values of T it varies linearly with the inverse of T and for large values of T it exhibits a quasi-exponential behavior (as expected). The exponential behavior may be explained considering that, if $T - In \gg (Re + In)/(1 - \lambda)$ the mean service cycle length will tend to be $E\{L_k\} = (Re + In)/(1 - \lambda)$ (see Case 1 in Appendix IV). In fact, $E\{L_k\}$ experiences insignificant variation for different values of T and traffic "shapes" (given that the arrival rate is kept constant and T is large). When T is increased, the service cycle length's probability distribution experiences little variation around its expected value, whereas the conditional

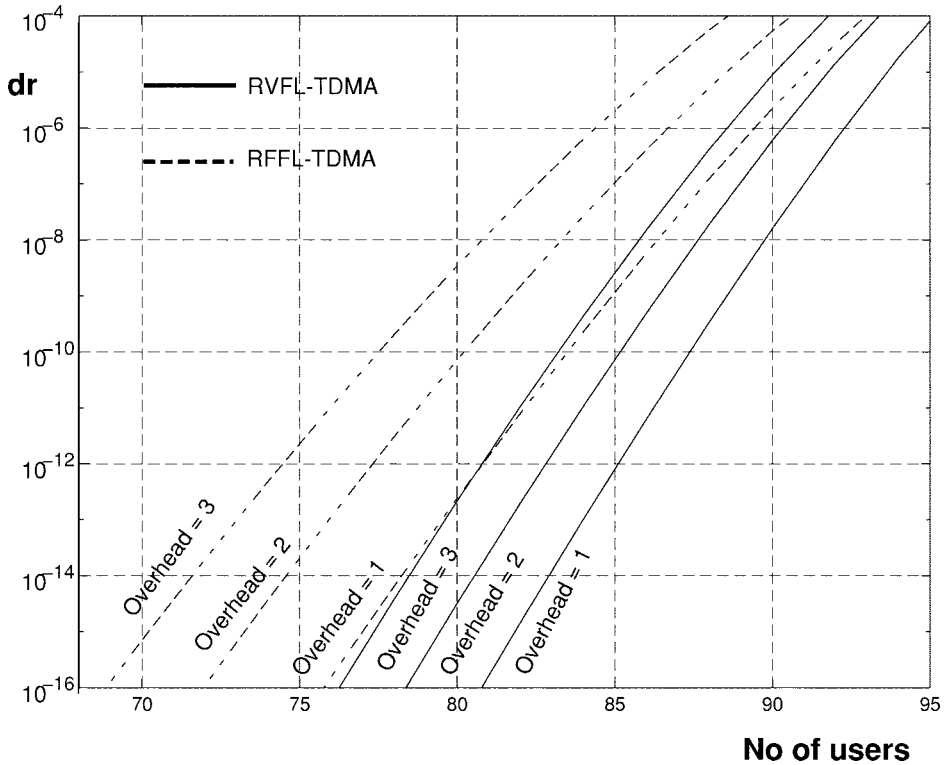

Fig. 11. Dropping rate under RVFL-TDMA and RFFL-TDMA schemes versus number of users; maximum delay tolerance $T = 100$ time slots.

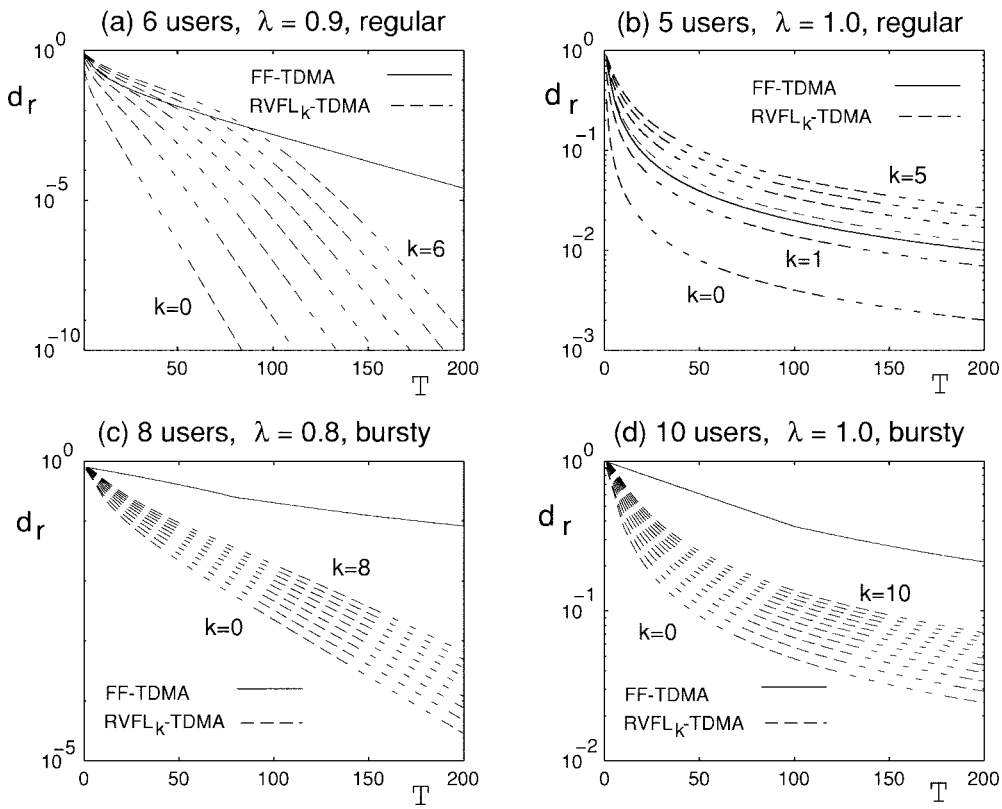

Fig. 12. Dropping rate (dr) versus maximum delay tolerance (T) under the FF-TDMA, RVFL$_k$-TDMA, and ICE-TDMA schemes for different traffic environments.

number of dropped cells decreases exponentially (as observed in the IVFL-TDMA and ICE-TDMA schemes). Therefore the contribution of service cycle lengths close to their expected value[3] to the dropping rate will decrease exponentially with T. The probability that the service cycle length be much

[3] See (8).

greater than the expected value decreases rapidly—and it seems exponentially—thus, for service cycle length close to $T+Re$ (causing the maximum number of cells to be dropped) increasing T would cause the event of being close to $T+Re$ to decrease as rapidly as the service cycle length probability distribution (that is, exponentially), meanwhile (for $\lambda < 1$) the number of cells dropped has little variation.[4] Therefore, the contribution to the dropping rate from service cycle lengths close to $T+Re$ will also tend to decrease exponentially with T, although it may be at a different rate. For T large, the term with lower exponential decay rate will dominate and the total dropping rate will vary exponentially with T.

The inversely linear behavior may be explained by noting that when the maximum delay tolerance is reduced

$$T - In < \frac{Re + In - \overline{d}^{I}_{r/T-In}(T - In)}{1-\lambda} < \frac{Re + In}{1-\lambda}$$

the service cycle length will tend to be inside the interval $\langle T - In, T + Re\rangle$ where the conditional number of dropped cells are usually dominated by the term $\lambda(L_{k-1} - T + In)$ (see Case 2 in Appendix IV). The dropping rate will be tightly lower bounded by (14) which is almost inversely linear for small values of T. In this scenario the dropping rate will be dominated by the arrival rate and frame overhead and will not vary significantly with the traffic "shape" or variance. The dropping rate function will have lost its exponential behavior due to the overhead period. Therefore, it may be said that in this region the overhead period produces its maximum degrading effect. The region where the linear function may be applied increases with the overhead period ($Re + In$) and/or the arrival rate. This implies that the difference between the dropping rate induced by two different traffic streams with the same arrival rate but different variance and "shapes" will tend to be smaller for larger overhead periods (as observed).

When λ increases, the region of T where the lower bound of (14) is applicable is increased. Outside this region, the dropping rate function does not necessarily behave exponentially but there is a second linear region; and only after $T - In \gg 1/(1 - r_d)$ the dropping rate function will behave exponentially.[5] In the limiting case ($\lambda = 1$), for small T [such that $\overline{d}^{I}_{r/T-In}(T - In) < Re + In$] the dropping rate will be dominated by the arrival rate and be close to the lower bound of (14), which for small T is close to $(Re + In)/(T + Re)$. When T increases [such that $\overline{d}^{I}_{r/T-In}(T - In) > Re + In$][6] the dropping rate will also depend on the variance (σ_I^2) whose degrading effect will be added to the one caused by the overhead. Thus, the dropping rate function will never reach a zone of exponential behavior and will always be (lossly) lower bounded by $(Re + In)/(T + Re)$.[7] Whether the overhead or the variance dominates the dropping rate will depend of their relatives values.

Summarizing the previous observations for the ICE-TDMA and RVFL-TDMA schemes, it may be seen that for large T, $\lambda < 1$, and small overhead period, the dropping rate exhibits an exponential behavior and depends on the arrival rate, variance and traffic shape. Increasing the overhead period and/or arrival rate and/or reducing T will cause the dropping rate to reduce its dependency on the traffic shape and variance. In the extreme case, the dropping rate function will enter a linear region and will be dominated by the arrival rate and overhead period (that is, different traffic patterns with the same arrival rates will induce almost the same dropping rate). A designer should work in the exponential region and treat the linear region as a degenerate case where the desired exponential behavior is lost without possibility of recovery. In addition to the complex expressions to compute the dropping rate, more simple expressions are presented that help a designer to quickly verify that he/she is working in the RVFL-TDMA scheme's "exponential" region [$T > 1/(1 - r_d)$ and $T \gg (Re + In)/(1 - \lambda)$].

A comparison between the RVFL-TDMA and RFFL-TDMA schemes shows that for the same amount of overhead, the RFFL-TDMA scheme significantly increases the induced system dropping rate, degrading the performance. This was expected due to the failure of the RFFL-TDMA scheme to adjust its frame length to the current traffic resulting in empty slots (wasted) when there is data to be transmitted or in frame lengths smaller than the optimal (the frame length should be as large as possible to reduce the effect of the frame overhead).

A comparison between the RVFL-TDMA with contention free reservation period (RVFL$_N$-TDMA) and the FF-TDMA shows that no one scheme outperforms the other in all cases; the formulas developed in this paper can be used to identify the best one for a particular case. In general, the FF-TDMA scheme may outperform the RVFL$_N$-TDMA scheme in situations where the performance degradation due to the frame overhead in the RVFL$_N$-TDMA scheme is more significant than the degradation under the static FF-TDMA scheme due to its failure to allocate efficiently dynamic (bursty) traffic. The overhead period dominates the dropping rate function in the linear region, as explained before. Therefore, when the traffic is regular with a total arrival rate close to one, the overhead period large, and/or the maximum delay tolerance small ($T < (Re+In)/(1-\lambda)$) the percentage of the server capacity that is wasted in reservations under the RVFL$_N$-TDMA scheme may be more significant than the performance degradation under the static FF-TDMA scheme, therefore favoring the latter. On

[4] For T large, $\overline{d}^{I}_{r/T-In}(T - In)$ converges to a constant value [equal to $N(1)/(1 - \lambda)$]. This is also intuitive since at the beginning of the service cycle there is low tolerance to burstiness. After the initial cells are dropped and for $\lambda < 1$, the difference between the cumulative arrivals and the survivor's function is expected to be large so that the system may absorb some bursty arrivals. Thus, after some point, increasing the value of T will not affect significantly the number of cells dropped.

[5] The second linear region may be explained since $\overline{d}^{I}_{r/T-In}(T - In)$ has not converged to a constant value yet. The quantity $\overline{d}^{I}_{r/T}(T)$ does not depend on the overhead length but it is computed for the IVFL-TDMA scheme. Since (under our assumptions) the IVFL-TDMA and ICE-TDMA schemes induce the same dropping rate, the linear region under both schemes is the same. Thus, for $T < 1/(1 - r_d)$ both schemes are in the linear region and it may be concluded that the quantity $\overline{d}^{I}_{r/T}(T)$ has not converged to a constant value yet.

[6] For $\lambda = 1$, $\overline{d}^{I}_{r/T-In}(T - In)$ does not converges to a finite value as $T \to +\infty$.

[7] For large values of T and $\lambda < 1$, the lower bound of (14) becomes negative (meaningless). But for $\lambda = 1$ the lower bound is always positive.

the other hand, more dynamic (bursty) traffic as well as greater maximum delay tolerance and/or arrival rates lower than one will favor the RVFL$_N$-TDMA scheme over the FF-TDMA scheme.

Finally, both schemes (RVFL$_N$-TDMA and FF-TDMA) are far from the optimal, so there is room for significant improvement using techniques as for example piggy-backing of arrival information, or arrival times estimation.

Appendix I
Closed-Form Expression for the Cell Dropping Rate as a Function of the Maximum Delay Tolerance Under the ICE-TDMA Scheme

A. Computation of P_{ij}

Let a_k be the number of cells arrived at t_k^+ as explained in Section II. Let $l_\mu = P\{a_k = \mu\}$ for $\mu = 0, \ldots, n$ where $n < T$ and l_μ is assumed to be independent of k. The following cases are considered.

Case 1: $i = 0$. If $j \geq 2$ it is impossible that $i = 0$. If $j = 1$, since the system is busy, the only possibility is that $a_k = 0$. If $j = 0$ two possibilities exist, depending on whether there was one arrival (system busy) or zero (system empty)

$$P_{ij} = \begin{cases} 0, & \text{if } j \geq 2 \\ l_0, & \text{if } j = 1 \\ l_0 + l_1, & \text{if } j = 0. \end{cases}$$

Case 2: $1 \leq i \leq T-2$. The system is busy so $P_{ij} = P\{a_k = i+1-j\} = l_{i+1-j}$

$$P_{ij} = \begin{cases} l_{i+1-j}, & \text{if } j \leq i+1 \\ 0, & \text{elsewhere.} \end{cases}$$

Case 3: $i = T-1$. Here it is possible to have had $j + a_k - T$ discarded cells. Thus, $P_{ij} = P\{j + a_k \geq T\}$

$$P_{ij} = \begin{cases} 0, & \text{if } 0 \leq j < T-n-1 \\ \displaystyle\sum_{d=T-j}^{n} l_d, & \text{if } T-n \leq j. \end{cases}$$

B. Computation of $\overline{\mathbf{\Pi}}$ (Steady-State Probability Distribution)

$\overline{\mathbf{\Pi}}$ can be easily computed from the equation $\mathbf{P}\overline{\mathbf{\Pi}} = \overline{\mathbf{\Pi}}$. But, since a closed-form solution is desirable to analyze the qualitative behavior of the system, a different approach can be followed.

Let x_i be a sequence defined as follows:

$$\begin{aligned} x_i &= 0 \qquad \text{for } i < 0 \\ x_0 &= 1 \\ x_1 &= \frac{1 - l_0 - l_1}{l_0} \\ x_i &= \frac{(1-l_1)x_{i-1} - l_2 x_{i-2} - \cdots - l_{n-1}x_{i-(n-1)} - l_n x_{i-n}}{l_0} \\ &\qquad \text{for } i \geq 2. \end{aligned}$$

It is easy to see that $\overline{\mathbf{x}} = (x_0, x_1, x_2, \ldots, x_{T-1})^t$ is a solution to the equation $\mathbf{P}\overline{\mathbf{x}} = \overline{\mathbf{x}}$. Then it is obvious that $\overline{\mathbf{\Pi}} = \overline{\mathbf{x}}/y_T$ where $y_T = \sum_{j=0}^{T-1} x_j$.

Let $X(z)$ be the Z-transform of x_i

$$\begin{aligned} X(z) &= \frac{l_0 + (l_0 x_1 + l_1 - 1)z^{-1}}{l_0 + (l_1 - 1)z^{-1} + l_2 z^{-2} + l_3 z^{-3} + \cdots + l_n z^{-n}} \\ &= \frac{l_0(1 - z^{-1})}{l_0 + (l_1 - 1)z^{-1} + l_2 z^{-2} + l_3 z^{-3} + \cdots + l_n z^{-n}} \\ &= \frac{l_0}{D(z)} \end{aligned}$$

where

$$\begin{aligned} D(z) = {} & l_0 + (l_0 + l_1 - 1)z^{-1} + (l_0 + l_1 + l_2 - 1)z^{-2} \\ & + \cdots + (l_0 + l_1 + l_2 + \cdots + l_{n-1} - 1)z^{-(n-1)}. \end{aligned}$$

From this expression $x(i)$ and $\overline{x}$ are easily computed.

To compute y_T the sequence $y_i = \sum_{i'=0}^{i-1} x_{i'}$ is used. It is clear that $y_i = x_{i-1} + y_{i-1}$ for all $i \geq 1$ and zero elsewhere; so taking y_i's Z-transform $Y(z)$

$$\begin{aligned} Y(z) &= z^{-1}Y(z) + z^{-1}X(z) \\ Y(z) &= \frac{l_0 z^{-1}}{(1 - z^{-1})D(z)}. \end{aligned}$$

Thus $Y(z)$, y_T, and $\overline{\Pi}$ are obtained.

C. Computation of the Dropping Rate $\mathbf{d_r}(\mathbf{T})$ (Cells/Time-Slot)

$$\begin{aligned} d_r(T) &= E\{\#\text{ cells dropped at } t_k^+\} \\ &= \sum_{j=1}^{n-1} jP\{j \text{ cells dropped at } t_k^+\} \\ &= \sum_{j=1}^{n-1} j \sum_{i=j+1}^{n} l_i \prod\nolimits_{T+j-i} \\ &= \sum_{u=1}^{n-1} \sum_{j=1}^{n-u} j l_{u+j} \prod\nolimits_{T-u} \\ &= \sum_{u=1}^{n-1} \sigma_u \prod\nolimits_{T-u} \end{aligned}$$

where $\sigma_u = \sum_{j=1}^{n-u} j l_{u+j}$, and since $\prod_i = x_i / y_T$

$$d_r(T) = \frac{\sigma_1 x_{T-1} + \sigma_2 x_{T-2} + \cdots + \sigma_{n-1} x_{T-(n-1)}}{y_T} = \frac{s_T}{y_T}.$$

The Z-transform of s_T is $S(z) = N(z)X(z)$, where $N(z) = (\sigma_1 z^{-1} + \sigma_2 z^{-2} + \sigma_3 z^{-3} + \cdots + \sigma_{n-1} z^{-(n-1)})$. Finally the dropping rate is given by

$$d_r(T) = \frac{\mathcal{Z}^{-1}\{N(z)X(z)\}}{\mathcal{Z}^{-1}\{Y(z)\}} = \frac{\mathcal{Z}^{-1}\left\{l_0 \dfrac{N(z)}{D(z)}\right\}}{\mathcal{Z}^{-1}\{Y(z)\}}.$$

Thus a closed-form solution is found. This method is computationally reliable and simple. It is reduced to the calculation of the impulse response of two infinite impulse response (IIR) filters. It provides for not only a quantitative evaluation of the dropping rate, but also describes its qualitative behavior by considering the poles of the filters. The following observations

can be made regarding the roots of $D(z)$ for $l_0 + l_1 < 1$ (i.e., for dropping rate different than zero).

i) Since all the coefficients of $D(z)$ are negative except for l_0, then for every $z_0 \in \mathcal{C}$, $Re[D(z_0)] \geq D(|z_0|)$ with equality only if $z_0 \in \mathcal{R}^+$. The sets $\mathcal{C}$ and $\mathcal{R}^+$ represent the set of complex numbers and the set of positive real numbers, respectively; the functions $Re[.]$ and $|.|$ represent the real part of a complex number and its absolute value, respectively.

ii) For every $r \in \mathcal{R}^+$ the function $D(r)$ is real and strictly increasing.

iii) If $r \to 0^+$ then $D(r) \to -\infty$; and if $r \to +\infty$ then $D(r) \to l_0 > 0$. Thus, $D(r)$ has one and only one real positive root, namely r_d.

iv) For any root r_i of $D(z)$ different than r_d, $|r_i| < r_d$.

Proof: Consider there is a root different than r_d such that $|r_i| \geq r_d$. From iii) r_i is not real positive, so applying i) as inequality (equality only holds for real positive numbers): $Re[D(r_i)] > D(|r_i|) \geq D(r_d) = 0$. The last two equalities came from ii) and iii), respectively. Finally, there is a contradiction because $D(r_i)$ is suppose to be equal to zero, but its real part is greater than zero. Thus, the initial assumption that there exists a root r_i of $D(z)$ such that $|r_i| \geq r_d$ is false. □

From all the above, it is concluded that the dominant pole of both filters will be r_d (real and positive). Also, it should be noted that

$$N(z) = \frac{z^{-1}[D(z) + \lambda - 1]}{1 - z^{-1}}$$

where λ be the mean arrival rate: $\lambda = E\{a_k\} = \sum_{\mu=0}^{n} \mu l_\mu$. Based on the previous relation (and its derivatives) it is easily shown that

$$\begin{aligned} D(1) &= 1 - \lambda, \\ D'(r_d) &= N(r_d) + (1 - r_d)|N'(r_d)|, \\ N(r_d) &= \frac{1 - \lambda}{1 - r_d}. \end{aligned}$$

Additionally, using the definition of $N(z)$ it may be verified that

$$N(1) = \frac{E\{a_k^2\} - E\{a_k\}}{2}, \qquad |N'(1)| = \frac{E\{a_k^3\} - E\{a_k\}}{6}.$$

Let $|r_s|$ be the absolute value of r_s [the root of $D(z)$ with the second largest absolute value]; thus for $r_d \neq 1$ and $T \gg 1/(r_d - |r_s|)$

$$\begin{aligned} \mathcal{Z}^{-1}\left\{\frac{l_0 z^{-1}}{(1 - z^{-1})D(z)}\right\} &\approx \frac{l_0}{D(1)} - \frac{l_0 r_d^T}{(1 - r_d) r_d D'(r_d)} \\ \mathcal{Z}^{-1}\left\{\frac{l_0 N(z)}{D(z)}\right\} &\approx \frac{l_0 N(r_d) r_d^T}{r_d D'(r_d)} \\ d_r(T) &\approx \frac{N(r_d) r_d^{T-1}}{\dfrac{D'(r_d)}{D(1)} - \dfrac{r_d^{T-1}}{1 - r_d}}. \end{aligned}$$

After some manipulation, the above expression becomes

$$d_r(T) \approx \frac{N(r_d) r_d^{T-1}}{\dfrac{1 - r_d^{T-1}}{1 - r_d} + \dfrac{|N'(r_d)|}{N(r_d)}}. \tag{9}$$

This expression allows to analyze the behavior of $d_r(T)$. Four cases are considered.

Case 1: $\lambda < 1, T < 1/(1 - r_d)$. It is known that $D(0^+) \to -\infty$, and $D(1) = 1 - \lambda > 0$. Thus the only real root of $D(z)$ (the dominant pole) will be $r_d < 1$. The closer λ to one and/or the greater the variance, the closer r_d to one. For values of $T - 1 \ll 1/(1 - r_d)$, $1 - r_d^{T-1} \approx (T - 1)(1 - r_d)$ and the dropping rate may be approximated by

$$d_r(T) \approx \frac{N(r_d) r_d^{T-1}}{T - 1 + \dfrac{|N'(r_d)|}{N(r_d)}}.$$

In this interval $(T < 1/(1 - r_d))$ and for values of r_d close to one, the dropping rate will be dominated for a inversely linear function of T.

Case 2: $\lambda < 1, T > 1/(1 - r_d)$. As explained before, the only real root of $D(z)$ (the dominant pole) will be $r_d < 1$. For values of $T \gg 1/(1 - r_d)$, $1 - r_d^{T-1} \approx 1$ and the dropping rate (9) may be approximated by

$$d_r(T) \approx \left\{\frac{1 - \lambda}{1 + (1 - r_d)\dfrac{|N'(r_d)|}{N(r_d)}}\right\} r_d^{T-1}.$$

Note that if r_d is close to one (λ close to one) the above expression can be simply written as $d_r(T) \approx (1 - \lambda) r_d^{T-1}$.

Therefore it can be concluded that the dropping rate as a function of the maximum delay tolerance (T) presents initially an inversely linear behavior and after that it presents an exponential behavior.

Case 3: $\lambda = 1$. Since $D(1) = 1 - \lambda = 0$, $r_d = 1$. Equation (9) was derived assuming $r_d \neq 1$ and should be rewritten for this particular case since $Y(z)$ has now a double root in $z = 1$. After the necessary manipulations, the result is the same obtained in the Case 1 when r_d approaches one. Therefore, for all T

$$d_r(T) \approx \frac{N(1)}{T - 1 + \dfrac{|N'(1)|}{N(1)}}.$$

But in this case

$$\begin{aligned} N(1) &= \frac{E\{a_k^2\} - E\{a_k\}}{2} = \frac{\sigma_l^2 + \lambda^2 - \lambda}{2} = \frac{\sigma_l^2}{2} \\ |N'(1)| &= \frac{E\{a_k^3\} - E\{a_k\}}{6} = \frac{m_l^{(3)} + 3\sigma_l^2 \lambda + \lambda^3 - \lambda}{6} \\ &= \frac{m_l^{(3)} + 3\sigma_l^2}{6} \end{aligned}$$

where σ_l^2 and $m_l^{(3)}$ represent the second and third central moment of the random variable a_k, respectively. For example, $m_l^{(3)} = E\{(a_k - E\{a_k\})^3\}$. The probability mass function of a_k is defined by l_μ (i.e., $P\{a_k = \mu\} = l_\mu$). Replacing these last identities in the above expression gives finally

$$d_r(T) \approx \frac{\sigma_l^2}{2\left(T + \dfrac{m_l^{(3)}}{3\sigma_l^2}\right)}.$$

Note that for T greater than $m_l^{(3)}$ the above expression can be written simply as $d_r(T) \approx \sigma_l^2/2T$. Therefore, for large values of T, the dropping rate will depend only in the ratio between the variance and the maximum delay tolerance.

Case 4: $\lambda > 1$. $D(1) = 1 - \lambda < 0$ and if $r \to +\infty$ then $D(r) \to l_0 > 0$ then for continuity there exist some $r_d > 1$ such that $D(r_d) = 0$. This means that the dominant pole will be $r_d > 1$. For values of $T-1 \ll 1/(r_d-1)$ the dropping rate may be approximated to the expression derived in Case 1. For $T-1 \gg 1/(r_d-1)$, r_d^{T-1} will be greater that any other term in (9) resulting in $d_r(T) \approx \lambda - 1$ [independent on the second and third moment, the shape of $D(z)$ and the maximum delay tolerance (T)].

Thus, the dropping rate as a function of T and the traffic characteristics (l_μ) has been calculated and its qualitative behavior has been analyzed.

Appendix II
Computation of the Function $P_j(\epsilon)$

Since $\{A_j(\tau)\}_{\tau=0}^{j}$ is a cumulative arrival process (see Section III-A) with independent increments, $A_j(\tau') = A_1(1) + A_{j-1}(\tau'-1)$ for $1 \le \tau' \le j$. Let τ'' be equal to $\tau'-1$. Then

$$A_j(\tau') - \tau' = [A_{j-1}(\tau'') - \tau''] + A_1(1) - 1,$$

and

$$\max_{1\le\tau'\le j} A_j(\tau') - \tau' = A_1(1) - 1 + \max_{0\le\tau''\le j-1} A_{j-1}(\tau'') - \tau''.$$

By employing the above

$$\begin{aligned} m(j) &= A_1(1) - 1 + \max\left\{0, \max_{1\le\tau''\le j-1} A_{j-1}(\tau'') - \tau''\right\} \\ &= A_1(1) - 1 + \max\left\{0, \max_{1\le\tau''\le j-1} A_j(\tau'') - \tau''\right\} \\ m(j) &= A_1(1) - 1 + \max\{0, m(j-1)\} \end{aligned}$$

thus

$$\begin{aligned} P\{m(j) = \epsilon\} = \sum_{\mu=0}^{n} & P\{A_1(1) = \mu\} \\ & \cdot P\{\max\{0, m(j-1)\} = \epsilon + 1 - \mu\} \end{aligned}$$

and since $P\{\max\{0, m(j-1)\} = \epsilon'\} = P_{j-1}(\epsilon')$, then

$$P\{m(j) = \epsilon\} = \sum_{\mu=0}^{n} P\{A_1(1) = \mu\} P_{j-1}(\epsilon + 1 - \mu).$$

Finally

$$P_j(\epsilon) = \begin{cases} P\{m(j) = \epsilon\}, & \text{if } \epsilon \ge 1 \\ P\{m(j) = 0\} + P\{m(j) = -1\}, & \text{if } \epsilon = 0 \\ 0, & \text{elsewhere} \end{cases} \tag{10}$$

$$= \begin{cases} \displaystyle\sum_{\mu=0}^{\min\{n,\,\epsilon+1\}} l_\mu P_{j-1}(\epsilon + 1 - \mu), & \text{if } \epsilon \ge 1 \\ l_0 P_{j-1}(0) + l_0 P_{j-1}(1) + l_1 P_{j-1}(0), & \text{if } \epsilon = 0 \\ 0, & \text{elsewhere.} \end{cases} \tag{11}$$

This recurrent formula and the fact that $P_0(\epsilon) = \delta_\epsilon$ [i.e. zero always except at $P_0(0) = 1$] are used to calculate $P_j(\epsilon)$ and then $d_{r/j}^{I}(T)$.

Appendix III
Dropping Rate Under the FL System

Let $\hat{A}_k(\tau)$ and $\hat{B}_k(\tau)$ be defined as before (Sections III and IV). Note that since in a RFFL-TDMA scheme there may be "remaining" cells from the previous services cycles, the initial value of $\hat{B}_k(\tau)$ may not be zero as before but equal to

$$\hat{B}_k(0) = \max\left\{0, \hat{B}_{k-1}(L_f) + Re + In - L_f\right\}.$$

Note that $\hat{B}_k(0)$ is completely defined by $\hat{B}_{k-1}(0)$ and the arrivals during the $(k-1)$th service cycle. Since the arrivals are assumed to be memoryless, $\{\hat{B}_k(0)\}$ is a discrete Markov chain with transition probabilities

$$P_{ij}^{FL} = P\left\{\hat{B}_k(0) = i / \hat{B}_{k-1}(0) = j\right\}.$$

The number of cells waiting for slot assignment τ slots into the $(k-1)$th service cycle is equal to the sum of the $\hat{B}_{k-1}(0)$ cells remaining at the beginning of the previous service cycle plus the $\hat{A}_{k-1}(\tau)$ new arrivals. The number of surviving cells τ slots into the $(k-1)$th service cycle, $\hat{B}_{k-1}(\tau)$, will not be limited by a line of the type $f_\tau = \tau + T - L_{k-1}$ as before (Section III-B, Fig. 4), but by a more complex one, as computed below and shown in Fig. 13.

Let f_τ^{FL} denote the maximum possible number of surviving cells up to time τ. If f_τ^{FL} is expressed as follows:

$$f_\tau^{FL} = (L_f - Re - In)\eta_\tau + \xi_\tau$$

where η_τ is an integer and $1 \le \xi_\tau \le L_f - Re - In$, then it is clear that the last of these f_τ^{FL} cells would be served at the $(k+\eta_\tau)$th service cycle. For this cell to be completely served it will have to wait the $L_f - Re - \tau$ time slots necessary to end the $(k-1)$th service cycle plus the $(1+\eta_\tau)(Re+In)$ slots of overhead periods plus f_τ^{FL} time slots. This time must be less than T time slots, resulting in the following condition:

$$\eta_\tau L_f + \xi_\tau \le \tau + T - L_f - In.$$

Since f_τ^{FL} is the maximum possible number of surviving cells, η_τ and ξ_τ must be assigned the maximum possible values, therefore

$$\begin{aligned} \eta_\tau &= \left\lfloor \frac{\tau + T - L_f - In - 1}{L_f} \right\rfloor \\ \xi_\tau &= \min\{\tau + T - (1+\eta_\tau)L_f - In,\, L_f - Re - In\} \end{aligned}$$

where $\lfloor x \rfloor$ represents the greater integer lower than or equal to x. The first equation holds since ξ_τ is at least one. The second equation holds since ξ_τ is (by definition) at most $L_f - Re - In$. These equations define f_τ^{FL} as a nondecreasing sequence that alternates periods of unit increments (for $L_f - Re - In$ time slots) with periods of nonincrements (for $Re + In$ time slots), and so on. Let β_τ represent the amount of increment of the sequence f_τ^{FL}. β_τ is one (zero) if the function f_τ^{FL} has

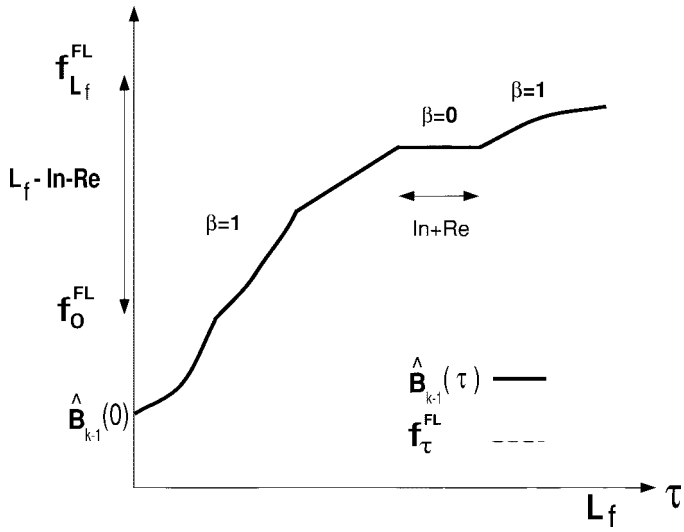

Fig. 13. Number of "surviving" cells $\hat{B}_{k-1}(\tau)$ among the cells arrived up to time $t^g_{k-1}+\tau$ for the RFFL-TDMA scheme.

increased (not increased) at time τ, that is, $\beta_\tau = f^{FL}_\tau - f^{FL}_{\tau-1}$ (see Fig. 13).

To evaluate the dropping rate $d^{FL}_r(T)$, the following procedure is used. First, the steady-state probability distribution function of $\{\hat{B}_k(0)\}$, namely $\prod^{FL}_B$ is calculated. Second, $\overline{d}^{FL}_{r/B}$ the conditional expected number of cells dropped at the beginning of the present frame (kth) given that the number of surviving cell ($\hat{B}_{k-1}(0)$) at the beginning of the previous frame [$(k-1)$th] is equal to B is calculated. Third, the dropping rate is computed from the following expression:

$$d^{FL}_r(T) = \frac{\sum_{B=0}^{f^{FL}_0} \overline{d}^{FL}_{r/B} \prod^{FL}_B}{L_f}. \tag{12}$$

A. Computation of $\prod^{FL}_i$

Let $PB^{FL}_\tau(i,j) = P\{\hat{B}_{k-1}(\tau) = i/\hat{B}_{k-1}(0) = j\}$ similar as before (Section III-B); then it follows:

$$PB^{FL}_\tau(i,j) = \begin{cases} \sum_{\mu=0}^{n} l_\mu PB^{FL}_{\tau-1}(i-\mu, j), & \text{if } i < f^{FL}_\tau \\ \sum_{\mu=0}^{n}\left(\sum_{\epsilon=\mu}^{n} l_\epsilon\right) PB^{FL}_{\tau-1}(i-\mu, j), & \text{if } i = f^{FL}_\tau \\ 0, & \text{elsewhere} \end{cases}$$

with the initial conditions

$$PB^{FL}_0(i,j) = \begin{cases} 1, & \text{if } i = j \\ 0, & \text{elsewhere.} \end{cases}$$

Using this recurrent formula, $PB^{FL}_{L_f}(i,j)$ is computed and then

$$P^{FL}_{ij} = \begin{cases} PB^{FL}_{L_f}(i + L_f - Re - In), & \text{if } i \geq 1 \\ \sum_{i'}^{L_f - Re - In} PB^{FL}_{L_f}(i', j), & \text{if } i = 0. \end{cases}$$

The matrix $\langle P^{FL}_{ij}\rangle$ with dimensions $f^{FL}_0 \times f^{FL}_0$ is used to compute $\prod^{FL}_B = P\{\hat{B}_k(0) = B\}$.

B. Computation of $\overline{d}^{FL}_{r/B}$

A similar approach to the one followed in Section III-A and Appendix II is employed to compute $\overline{d}^{FL}_{r/B}$. Let the auxiliary quantity $\hat{m}^{FL}_k(\tau)$ be redefined as

$$\hat{m}^{FL}_k(\tau) = \max_{L_f - \tau \leq \tau' \leq L_f} \left\{\left[\hat{A}_{k-1}(\tau') - \hat{A}_{k-1}(L_f - \tau)\right] - \left[f^{FL}_{\tau'} - f^{FL}_{L_f - \tau}\right]\right\}.$$

Then, it is straightforward to show that the number of dropped cells at t^g_k is equal to

$$\hat{d}^{FL}_{r,k} = \max\left\{0, \hat{m}^{FL}_k(L_f) + \hat{B}_{k-1}(0) - f^{FL}_0\right\}$$

and also

$$\hat{m}^{FL}_k(\tau) = \max\left\{0, \hat{m}^{FL}_k(\tau - 1) + a_{L_f - \tau + 1} - \beta_{L_f - \tau + 1}\right\}$$

where $a_{L_f - \tau + 1} = \hat{A}_{k-1}(L_f - \tau + 1) - \hat{A}_{k-1}(L_f - \tau)$, and $\beta_{L_f - \tau + 1} = f^{FL}_{L_f - \tau + 1} - f^{FL}_{L_f - \tau}$ represent the number of cell arrivals and the amount of increment of the sequence f^{FL}_τ at time $t^g_{k-1} + L_f - \tau + 1$, respectively.

Let $P^{FL}_j(\epsilon) = P\{\hat{m}^{FL}_k(j) = \epsilon\}$; then the following recurrent formula holds:

$$P^{FL}_j(\epsilon) = \begin{cases} \sum_{\mu=0}^{n} l_\mu P^{FL}_{j-1}(\epsilon + \gamma_j - \mu), & \text{if } \epsilon \geq 1 \\ l_0 P_{j-1}(\gamma_j - 1) + l_0 P_{j-1}(\gamma_j) \\ \quad + l_1 P_{j-1}(\gamma_j - 1), & \text{if } \epsilon = 0 \\ 0, & \text{elsewhere} \end{cases}$$

with initial conditions

$$P^{FL}_0(i) = \begin{cases} 1, & \text{if } i = 0 \\ 0, & \text{elsewhere} \end{cases}$$

and where $\gamma_j = \beta_{L_f - j + 1}$; or similarly

$$\gamma_j = \begin{cases} 0, & \text{if } T - In - 1 - (\eta')L_f \leq j \\ & \quad \leq T + Re - (\eta')L_f \text{ for some } \eta' \text{ integer} \\ 1, & \text{elsewhere.} \end{cases}$$

Then, $\overline{d}^{FL}_{r/B}$ can be computed as follows:

$$\begin{aligned} \overline{d}^{FL}_{r/B} &= E\left\{\hat{d}^{FL}_{r,k}/\hat{B}_{k-1}(0) = B\right\} \\ &= \sum_{d=1}^{+\infty} d.P\left\{\hat{d}^{FL}_{r,k} = d/\hat{B}_{k-1}(0) = B\right\} \\ &= \sum_{d=1}^{+\infty} d.P\{\hat{m}^{FL}_k(L_f) = d + f^{FL}_0 - B\} \\ &= \sum_{d=1}^{+\infty} d.P^{FL}_{L_f}(d + f^{FL}_0 - B). \end{aligned}$$

Finally, the dropping rate is computed from $\overline{d}^{FL}_{r/B}$ and $\prod^{FL}_B$ using (12).

APPENDIX IV
ALTERNATIVE EXPRESSIONS, APPROXIMATIONS, AND ANALYSIS FOR THE DROPPING RATE INDUCED UNDER THE RVFL-TDMA SCHEME

The following expression may also be used for the calculation of $d_r^L(T)$ when $Re + In > 0$:

$$d_r^L(T) = \frac{Re + In}{E\{L_k\}} - (1 - \lambda) \tag{13}$$

where $E\{L_k\}$ and λ are the expected frame length and number of arrivals per time-slot (arrival rate), respectively.

Proof: Since cells are either dropped or served, the utilization (U), the dropping rate (d_r), and the arrival rate (λ) are related by: $U + d_r = \lambda$. Also, since a time slot is used either for reservation, or information, or cell transmission, then: $Re + In + UE\{L_k\} = E\{L_k\}$. Combining these two equations gives the above expression for $d_r^L(T)$. □

Equation (13), in general, is not numerically reliable since it requires the subtraction of two quantities that are too close to each other. For this reason it has not been used for the derivation of the numerical results. Nevertheless, it provides insight into the system behavior and it is used for the qualitative analysis of the system. From (13) the following lower bound may be found for the L system:

$$d_r^L(T) \geq \frac{Re + In}{Re + In + \lambda(T - In) - d^I_{r/T-In}(T - In)} - (1 - \lambda). \tag{14}$$

Equation (14) is derived using the fact that $E\{L_k\} \leq Re + In + \lambda(T - In) - d^I_{r/T-In}(T - In)$; the latter inequality is proved below.

Proof: The kth service cycle's length (L_k) is equal to the overhead period ($Re + In$) plus the arrivals over the interval $\langle t^g_{k-1}, t^g_k \rangle$ [see Fig. 2(b)] minus the number of cells dropped at time t^g_k (namely $\hat{d}_{r,k}$). Conditioned on that the previous service cycle's length (L_{k-1}) was equal to j, the expected number of arrivals over the interval $\langle t^g_{k-1}, t^g_k \rangle$ is simply λj and the expected number of cells dropped at t^g_k is equal to $\overline{d}^L_{r/j}(T)$, as derived in Section IV-A. Therefore, the expected service cycle length given that the previous service cycle length was j is given by

$$\begin{aligned} E\{L_k/L_{k-1} = j\} &= Re + In + \lambda j - \overline{d}^L_{r/j}(T) \qquad (15)\\ &= \begin{cases} Re + In + \lambda j - \overline{d}^I_{r/j}(T - In), & \text{if } j < T - In \\ Re + In + \lambda(T - In) - \overline{d}^I_{r/T-In}(T - In), & \text{if } T - In \leq j \leq T + Re \end{cases} \qquad (16) \end{aligned}$$

which is—as expected—a nondecreasing function in j. The nondecreasing property of $E\{L_k/L_{k-1} = j\}$ is obvious for $j \geq T - In$. For $j < T - In$ it follows from

$$\begin{aligned} &E\{L_k/L_{k-1} = j + 1\} - E\{L_k/L_{k-1} = j\} \\ &= \lambda - \left[\overline{d}^I_{r/j+1}(T - In) - \overline{d}^I_{r/j}(T - In)\right] \\ &= \lambda - \left[\lambda G_j(T - In) + \sum_{\mu=0}^{n-1} \sigma_\mu P_j(T - In - j - \mu)\right] \\ &= \lambda[1 - G_j(T - In)] - \sum_{\mu=0}^{n-1} \sigma_\mu P_j(T - In - j - \mu) \\ &= \lambda \sum_{i=0}^{T-In-j} P_j(i) - \sum_{i=T-In-n+1}^{T-In-j} \sigma_{T-In-j-i} P_j(i) \\ &\geq \sum_{i=0}^{T-In-j} (\lambda - \sigma_{T-In-j-i}) P_j(i) \\ &\geq 0. \end{aligned}$$

where (3) has been used along with the fact that $\lambda = \sigma_0 \geq \sigma_1 \geq \cdots \geq \sigma_{n-1}$.

Therefore, $E\{L_k/L_{k-1} = j\} \leq Re + In + \lambda(T - In) - \overline{d}^I_{r/T-In}(T - In)$ for all j. It immediately follows that

$$\begin{aligned} E\{L_k\} &= E\{E\{L_k/L_{k-1}\}\} \\ &\leq Re + In + \lambda(T - In) - \overline{d}^I_{r/T-In}(T - In) \end{aligned}$$

which completes the proof of (14). □

It is also interesting to analyze the drift of L_k. Let $D(j)$ be the drift of the L_k when $L_k = j$; that is, $D(j) = E\{L_k - L_{k-1}/L_{k-1} = j\}$. From (16), $D(j)$ is equal to

$$D(j) = \begin{cases} Re + In - (1 - \lambda)j - \overline{d}^I_{r/j}(T - In), & \text{if } j < T - In \\ Re + In + \lambda(T - In) - j - \overline{d}^I_{r/T-In}(T - In), & \text{if } j \geq T - In \end{cases} \tag{17}$$

which is not increasing in j (assuming $\lambda < 1$). Two cases may be considered.

Case 1: $D(T - In) < 0$, i.e.,

$$T - In > \frac{Re + In - \overline{d}^I_{r/T-In}(T - In)}{1 - \lambda}.$$

The value of j for which the drift is zero[8] (namely L_k^*) will be lower than $T - In$ and it will satisfy the equation

$$L_k^* = \frac{Re + In - \overline{d}^I_{r/L_k^*}(T - In)}{1 - \lambda}.$$

The service cycle length (L_k) will tend to be around $L_k^* < (Re + In)/(1 - \lambda)$. When T increases, L_k^* will also increase. It is interesting to notice that for $T - In \gg (Re + In)/(1 - \lambda)$, $\overline{d}^I_{r/L_k^*}(T - In) \approx 0$ [since $L_k^* \approx (Re + In)/(1 - \lambda) \ll T - In$], and therefore $L_k \approx (Re + In)/(1 - \lambda)$ which is a quantity independent of T. This is consistent with (13) since for T

[8] Strictly speaking j is a discrete variable and there may not be a discrete value of j such that the drift is zero. However, the drift function—$D(j)$—may be extrapolated for noninteger values and it is possible to find a value (L_k^*) for which $D(L_k^*) = 0$.

large, the dropping rate is small and therefore $E\{L_k\} = (Re+In)/((1-\lambda)+d_r^L(T)) \approx (Re+In)/(1-\lambda)$. Therefore, when $T-In \gg (Re+In)/(1-\lambda)$, the expected service cycle length will be close to $(Re+In)/(1-\lambda)$ and the service cycle length distribution around this value $((Re+In)/(1-\lambda))$ will not vary (significantly) when T is increased.

Case 2: $D(T-In) > 0$, i.e.,

$$T - In < \frac{Re + In - \overline{d}^I_{r/T-In}(T-In)}{1-\lambda}.$$

The value of j for which the drift is zero is equal to $L_k^* = Re+In+\lambda(T-In)-\overline{d}^I_{r/T-In}(T-In) > T-In$. Clearly, $T-In < L_k^* < T+Re$. When T decreases, L_k^* will tend to be closer to $T+Re$ than to $T-In$. The service cycle length will tend to be around L_k^*, that is, in the interval $\langle T-In, T+Re\rangle$, in which the conditional expected number of dropped cells (see Case 2 in Section IV-A) is equal to $\overline{d}^L_{r/j}(T) = \lambda(j-T+In)+\overline{d}^I_{r/T-In}(T-In)$. Therefore it may be seen that the number of cells dropped will depend on two different mechanisms. For large values of $Re+In$ and/or small values of $\overline{d}^I_{r/T-In}(T-In)$—and small values of T such that L_k^* is close to $(T+Re)$—the first term will be more significant that the second and dominate the dropping rate expression. Therefore, the dropping rate will depend more on the overhead length and arrival rate than on the particular "shape" of the traffic. Additionally, in this region the lower bound presented in (14) will be positive, approximately inversely linear, and increasingly tight[9]—when T decreases.

REFERENCES

[1] D. C. Cox, "Wireless network access for personal communications," *IEEE Commun. Mag.*, vol. 30, no. 12, pp. 96–115, Dec. 1992.

[2] I. M. Leslie, D. R. McAuley, and D. L. Tennenhouse, "ATM everywhere," *IEEE Network*, pp. 40–46, Mar. 1993.

[3] B. Walke, D. Petras, and D. Plassman, "Wireless ATM: Air interface and network protocols of the mobile broadband system," *IEEE Personal Commun. Mag.*, vol. 3, no. 4, pp. 50–56, Aug. 1996.

[4] D. Raychaudhuri and N. Wilson, "ATM-based transport architecture for multiservices wireless personal communication network," *IEEE J. Select. Areas Commun.*, vol. 12, pp. 1401–1414, Oct. 1994.

[5] K. Y. Eng, M. Karol, M. Veeraraghavan, E. Ayanoglu, C. B. Woodworth, P. Pancha, and R. A. Valenzuela, "A wireless broadband *ad-hoc* ATM local area network," *ACM Wireless Networks J.*, vol. 1, no. 2, pp. 161–174, Dec. 1995.

[6] P. Mermelstien, A. Jalali, and H. Leib, "Integrating services on wireless multiple access networks," in *Proc. ICC*, Mar. 1993, pp. 863–867.

[7] D. Petras, A. Kramling, and A. Hettich, "MAC protocol for wireless ATM: Contention free versus contention based transmission reservation request," in *Proc. PIMRC*, Taipei, Taiwan, Oct. 1996, pp. 903–907.

[8] M. Karol, Z. Liu, and K. Eng, "An efficient demand-assignment multiple access protocol for wireless packet (ATM) networks," *ACM Wireless Networks J.*, vol. 1, no. 4, pp. 267–279, Dec. 1995.

[9] A. Mahmoud, D. Falconer, and S. Mahmoud, "A multiple access scheme for wireless access to a broadband ATM LAN based on polling and sectored antennas," *IEEE J. Select. Areas Commun.*, vol. 14, pp. 596–608, May 1996.

[9] If the service cycle length distribution is mainly concentrated around L_k^* (inside the interval $\langle T-In, T+Re\rangle$) then only Case 2 in Section IV-A impacts on the dropping rate. The expected number of cells dropped in a service cycle will be approximately equal to $\lambda(L_k^*-T+In)+\overline{d}^I_{r/T-In}(T-In)$, and the expected service cycle length will be $\approx L_k^*$. Their ratio will determine the dropping rate. The result after simplifications is equal to the lower bound of (14).

[10] C.-S. Chang, K.-C. Chen, M.-Y. You, and J.-F. Chang, "Guaranteed quality of service wireless access to ATM networks," *IEEE J. Select. Areas Commun.*, vol. 15, pp. 106–118, Jan. 1997.

[11] N. Passas, L. Merakos, D. Skyrianoglou, F. Bauchot, G. Marmigere, and S. Decrauzat, "MAC protocol and traffic scheduling for wireless ATM networks," *ACM Mobile Networks Applicat. J* vol. 3, pp. 275–292, Sept. 1998.

[12] D. Bantz and F. Baucho, "Wireless LAN design alternatives," *IEEE Networks Mag.*, vol. 8, no. 2, pp. 43–53, Mar./Apr. 1994.

[13] S. S. Panwar *et al.*, "Optimal scheduling policies for a class of queues with customer deadlines to the beginning of service," *J. ACM*, pp. 832–844, 1988.

[14] G. Chen and I. Stavrakakis, "ATM traffic management with diversified loss and delay requirements," in *Proc. Infocom*, San Francisco, CA, Mar. 1996, pp. 1037–1044.

[15] J. R. Jackson, "Scheduling a production line to minimize tardiness," Management Sci. Rep., University of California, Los Angeles, Res. Rep. 43, 1955.

[16] C. L. Liu and J. W. Layland, "Scheduling algorithms for multiprogramming in a hard real time environment," *J. ACM*, pp. 46–61, Jan. 1973.

César Santiváñez (S'92) was born in Lima, Peru, in 1971. He received the B.S. degree (first class honors) and the Electrical Engineering degree from the Pontificia Universidad Catolica del Peru, Lima, in 1993 and 1994, respectively. He received the M.S. degree from Northeastern University, Boston, MA, in 1998 where he is currently pursuing the Ph.D. degree, both in electrical engineering.

From 1993 to 1994, he worked at INICTEL (Peruvian National Institute for Research in Telecommunications) conducting research in speech recognition. During 1994, he worked at COASIN PERU on internetworking projects. From 1995 to 1996, he worked as a Project Engineer at TELE2000, Peruvian first cellular service provider, in wireless data (CDPD) network's projects. Since 1996, he has been with the Communication and Digital Signal Processing Center at Northeastern University where he is currently a Research Assistant. His present research interests include multiaccess, routing, and QoS provision for mobile wireless communication networks.

Mr. Santiváñez was a Fulbright Scholar from 1996 to 1998. He received the best student paper award at MoMuc'98 Berlin, Germany, in 1998. He won a silver medal in the IV Iberoamerican Mathematics Olympics at HAVANA-CUBA as a member of the Peruvian delegation in April 1989. He was awarded a scholarship from the Peruvian Council for Science and technology (CONCYTEC) in 1989–1990 for tuition expenses. He is a member of the Phi Kappa Phi interdisciplinary honors society and el colegio de Ingenieros del Peru (Peruvian engineering professional society).

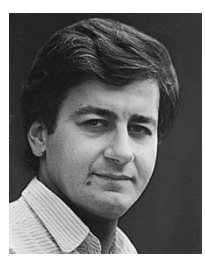

Ioannis Stavrakakis (S'84–M'88–SM'93) received the Diploma in electrical engineering from the Aristotelian University of Thessaloniki, Thessaloniki, Greece, in 1983, and the Ph.D. degree in electrical engineering from the University of Virginia, Charlottesville, in 1988.

In 1988, he joined the faculty of Computer Science and Electrical Engineering, University of Vermont, Burlington, first as an Assistant and then as an Associate Professor. Since 1994, he has been an Associate Professor of Electrical and Computer Engineering at Northeastern University, Boston, MA. His research interests are in stochastic system modeling, teletraffic analysis, and discrete-time queueing theory, with primary focus on the design and performance evaluation of broadband integrated services digital networks (B-ISDN).

Dr. Stavrakakis is a member of the IEEE Communications Society and the Technical Committee on Computer Communications. He has organized and chaired sessions and has been a technical committee member for conferences, such as GLOBECOM, ICC, and INFOCOM.